The soft-bodied biota of the Cambrian Series 2 Parker Quarry Lagerstätte of northwestern Vermont, USA

Giovanni Pari,[1] Derek E.G. Briggs,[2]* and Robert R. Gaines[3]

[1]44 Fairpark Drive, Ottawa, Ontario, K2G 6X8, Canada; <giovannipari@yahoo.com>
[2]Department of Earth and Planetary Sciences, and Yale Peabody Museum of Natural History, Yale University, New Haven, Connecticut, 06520, USA; <derek.briggs@yale.edu>
[3]Geology Department, Pomona College, Claremont, California, 91711, USA; <Robert.Gaines@pomona.edu>

Abstract.—A non-biomineralized arthropod, *Protocaris marshi*, was described from the lower Cambrian (Dyeran Series 2, Stage 4) of Parker's Cobble in northwestern Vermont in 1884. It represents the first fossil exhibiting Burgess Shale-type preservation to have been discovered. The locality was presumed to have been worked out and was not collected in a significant way for more than 100 years. Rediscovery of productive layers has yielded soft-bodied and lightly sclerotized taxa new to the locality, including the alga *Fuxianospora*, a possible priapulid, a radiodont, and a specimen tentatively assigned to *Herpetogaster*. New specimens of the sponge *Leptomitus zitteli*, the bivalved arthropod *Tuzoia*, and the chordate *Emmonsaspis cambrensis* provide additional information on those taxa, and multiple specimens allow a bivalved arthropod, *Vermontcaris montcalmi* new genus, new species, to be described. The primary mode of fossil preservation is as carbonaceous compressions. The Parker Quarry Lagerstätte complements the Kinzers Formation of Pennsylvania (also Series 2, Stage 4) in revealing the diversity of soft-bodied taxa on the southern margin of the paleocontinent Laurentia.

UUID: http://zoobank.org/2eb3ae7c-6579-403e-a9ab-654c05af4a1b

Introduction

Noah Parker discovered trilobites while quarrying slate near Saint Albans in northwestern Vermont in 1855 (Marcou, 1888). These remarkable fossils, first reported by James Hall (1859), are now known as *Mesonacis vermontanus*, *Olenellus thompsoni*, and *Bathynotus holopygus*. The trilobites from the locality have continued to merit attention (Whittington, 1989; Lieberman, 1999; Webster, 2009; Webster and Landing, 2016). Walcott's (1884) description of the non-biomineralized bivalved arthropod *Protocaris marshi* established the Parker Quarry as the first locality to yield a Burgess Shale-type soft-bodied fossil (Landing, 2007; Pari et al., 2021). Shaw (1954, p. 1041) reported that "the Noah Parker Quarry has been entirely quarried away," giving rise to the assumption that there was no longer scope for collecting soft-bodied fossils there (Briggs, 1976; Rigby, 1987; Conway Morris, 1993; Landing, 2007; Webster, 2009; Webster and Landing, 2016). The productive layers were rediscovered by GP in 2001 and have since yielded several new specimens of the trilobites and new soft-bodied fossils, including taxa previously unknown from the site (Pari et al., 2021) (Figs. 1–10).

Walcott's (1884) description and illustration of *Protocaris marshi* was appended to a report treating Cambrian faunas of

New Brunswick and Massachusetts. The description was reprinted in Walcott's (1886) account of the Cambrian faunas of North America, with some additional remarks on a possible relationship between *Protocaris* and the notostracan branchiopod *Triops* (then known as *Apus*). Walcott (1886) listed and described fossils from the Parker Quarry, including illustrations (pl. 11, figs. 4, 4a) of two fossils, which he referred to *Diplograptus* ? *simplex*. Resser and Howell (1938) argued that these specimens are likely to represent a chordate and one of them (Walcott, 1886, pl. 11, fig. 4a) was subsequently identified as such (Conway Morris and Caron, 2014). The other (Walcott, 1886, pl. 11, fig. 4) is an example of *Vermontcaris montcalmi* n. gen. n. sp., a new bivalved arthropod named and described here. Walcott identified a third 'soft-bodied' specimen (1886, pl. 11, fig. 5) as *Climacograptus* ? *emmonsi*, which Resser and Howell (1938) regarded as arthropodan and probably *Anomalocaris*. Briggs (1978b, 1979) rejected this interpretation, and the affinities of this specimen remain uncertain. Walcott (1886, pl. 2, figs. 2, 2a) also described and illustrated the sponge *Leptomitus zitteli*, which preserves soft tissue as dark carbonaceous material associated with the spicules. Finally, in his synopsis of the fauna of the lower Cambrian or *Olenellus* Zone, Walcott (1890) reproduced his figure of *Protocaris marshi* (pl. 81, fig. 6) and those of *Leptomitus zitteli* (pl. 49, figs. 1, 1a). He refigured the two specimens he previously identified as *Diplograptus* ? *simplex*, referring them to *Phyllograptus* ?? with a new species name *cambrensis* (pl. 59, figs. 3, 3a) and remarking on "the
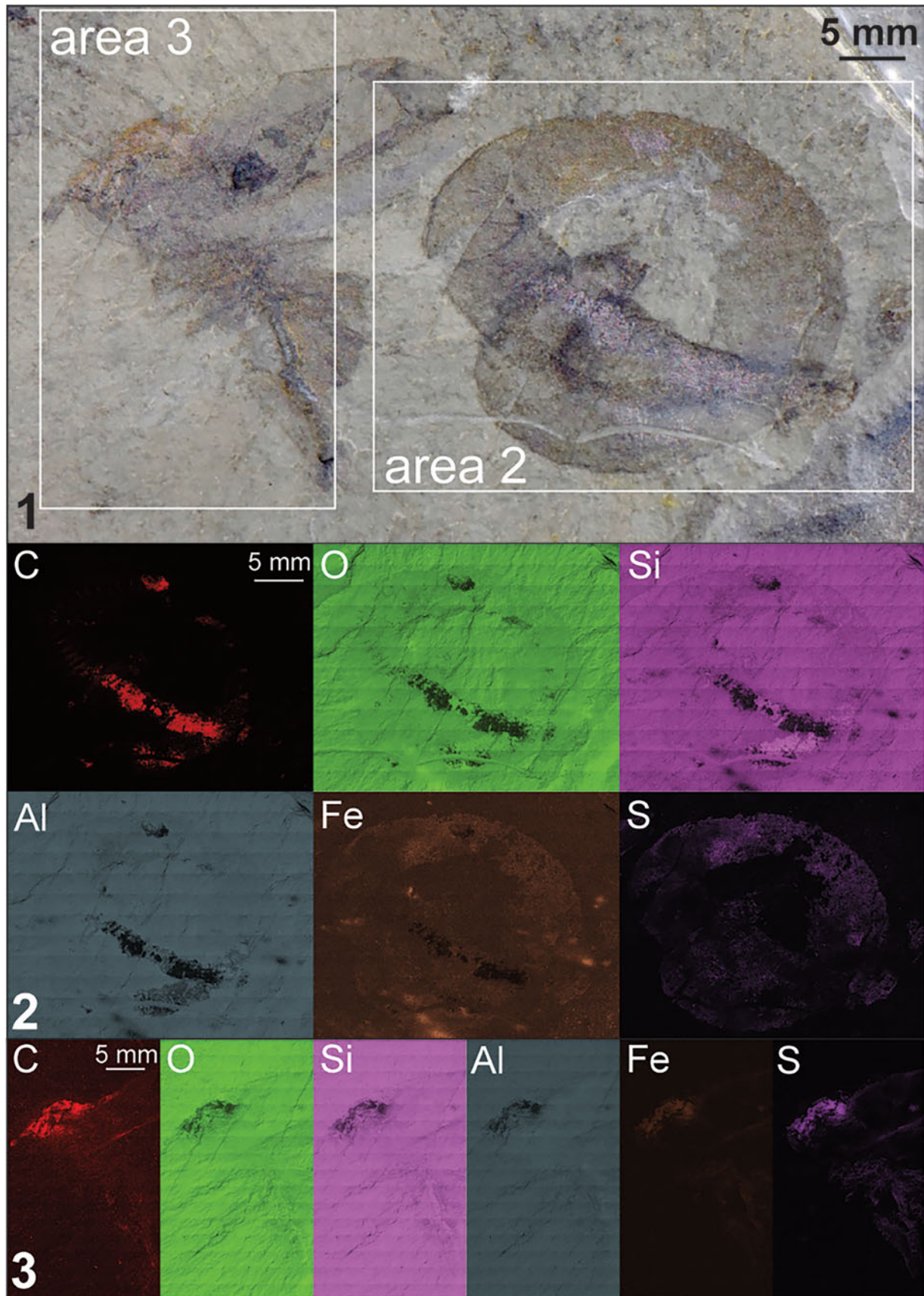
*Corresponding author

Figure 1. EDS elemental maps of ?*Ottoia* (YPM IP 239053) and *Vermontcaris montcalmi* n. gen. n. sp. (YPM IP 543321). (**1**) Photograph of YPM IP 239053 and YPM IP 543321, showing the areas mapped. (**2, 3**) Elemental maps showing the distribution of C, O, Al, Si, Fe, and S in areas (**2**) (YPM IP 239053) and (**3**) (YPM IP 543321).

imperfection of the material for study." Walcott also illustrated a specimen of *Tuzoia* (pl. 59, fig. 1) without description, the first record of this bivalved arthropod, noting it as "a problematical organic marking." Thus, the importance of the Parker Formation as a source of non-biomineralized fossils dates from 1884, and by 1890, 20 years before the first report of fossils from the more famous Burgess Shale (Walcott, 1911a), five soft-bodied or lightly sclerotized genera representing three different phyla had been discovered, even though only *Protocaris* and *Leptomitus* had been named and correctly assigned to a group.

New specimens collected from the Parker Quarry Lagerstätte (Pari et al., 2021) include representatives of all these soft-bodied and lightly sclerotized taxa except *Protocaris*, as well as the alga *Fuxianospora* and single examples of a stem ecdysozoan similar to *Ottoia*, a radiodontan appendage, and a possible cambroernid comparable to *Herpetogaster*, taxa previously unknown from the site. These soft-bodied and lightly sclerotized taxa are the subject of this paper. Rare shelly taxa have also been found, including trilobites, an obolid brachiopod and a hyolith (Pari et al., 2021). The Parker Formation biota is important among Burgess Shale-type faunas not only as the first reported, but also as one of the oldest (Dyeran Series 2, Stage 4) on the North American continent (Conway Morris, 1989; Hagadorn, 2002; Pari et al., 2021).

Locality and stratigraphic horizon

Fossils were collected from the Parker Quarry, Franklin County, Vermont, within the Parker Formation in the latter half of the 19th century (see Webster and Landing, 2016). The most significant material was recovered by Walcott in 1883 and 1884 (Walcott, 1885; see Yochelson, 1998). That original material was assigned to three US National Museum localities: 319g, 319m, and 25. Shaw (1954, p. 1040) considered 319g and 319m, both described by Walcott (1912b), to be "almost certainly the same," a view endorsed by Webster and Landing (2016). Confusion about the location of USNM 25, and by inference the total thickness of the productive layers of the Parker Quarry (Shaw, 1954; Webster and Landing, 2016), reflects an error in Walcott (1912b) where USNM 25 is recorded in the 'sandstone' unit above the Parker Quarry rather than in 'argillaceous shales' (Walcott, 1910). USNM 25 is the type locality for *Protocaris marshi* Walcott, 1884, and *Tuzoia polleni* Resser, 1929, both of which occur in poorly oxygenated mudstones characteristic of Burgess Shale-type preservation. Our own observations reject the possibility of soft-bodied fossil collections from the arenaceous dolomites that cap the productive, interbedded mudstone layers. Marcou's (1880, p. 24) view that "near the top of the quarry, the shale became sandy and slightly calcareous … It was in this interval that most of the trilobite specimens were found" (translated from French) is misleading. USNM localities 25 and 319m should be equated (Resser and Howell, 1938). Their faunas are virtually indistinguishable (Shaw, 1954) and similar to ours; they likely refer to a lost site (or nearby sites: Yochelson, 1998) on the south-western flank of Parker's Cobble where we have carried out our own excavations (44°44′N, 73°09′W). Under these assumptions, the productive layers of the Parker Quarry could not have exceeded 8–10 m and not extended to 18.3 m or even 27.4 m (Webster and Landing,

2016). The new fossils described here came from an interval of just 3 m within this larger thickness (Pari et al., 2021).

Webster and Landing (2016) provided a detailed review of the geology and stratigraphic setting of the Parker Quarry Lagerstätte within the Parker Formation (see also Ratcliffe et al., 2011). Determination of the biostratigraphic position of the fauna is hampered by the lack of an up-to-date taxonomic treatment of most of the trilobites, many of which are known only from northwestern Vermont. Webster and Landing (2016) tentatively correlated the Parker Quarry Lagerstätte with the *Bolbolenellus euryparia* Zone or overlying *Nephrolenellus multinodus* Zone of the Laurentian Cordilleran margin within Dyeran Series 2, Stage 4. The exceptionally preserved fossils of the Kinzers Formation of Pennsylvania likewise have been assigned to Series 2, Stage 4 (Skinner, 2005; Webster and Landing, 2016), older than the Burgess Shale, which falls in Miaolingian (formerly Series 3), Wuliuan.

Sedimentology

The mudstone-dominated strata of the Parker Formation at Parker's Cobble have undergone low-grade metamorphism resulting in a bedding-parallel cleavage, which facilitates splitting. Sedimentary features are largely obscured in the field by pyrite weathering, which stains surfaces with iron oxides, but they are clearly revealed in polished slabs (Pari et al., 2021). The soft-bodied fossils occur in claystone event beds that, combined with evidence for graded bedding and a lack of wave influence, indicate deposition from mud-rich flows below storm wave base (Pari et al., 2021). Trilobites occur in the same beds and in other mudstone lithologies, but they have not been observed in sandstone beds (Pari et al., 2021). The setting, near the foot of a major break in slope (Landing, 2007; Webster and Landing, 2016), is similar to that of the Burgess Shale at the base of the Cathedral Escarpment (Conway Morris, 1986; Aitken, 1997) and, as in the Burgess Shale, slump folds and other evidence of synsedimentary deformation are abundant in the ~3 m interval excavated for this study (Pari et al., 2021). The complete absence of evidence for bioturbation on bedding planes as well as polished cross-sections, and the enrichment in molybdenum in the fossil-bearing layers, suggest low oxygen levels (Pari et al., 2021).

EDS mapping (Fig. 1) of two little-weathered specimens in close proximity (Figs. 4.1, 9.9; Pari et al., 2021, fig. 2G) reveals areas preserved as a thin carbonaceous film, the primary mode of Burgess Shale-type preservation. The maps show that other elements are present on the surface of the fossils in proportions similar to the matrix. Most specimens of the new bivalved arthropod *Vermontcaris montcalmi* n. gen. n. sp. preserve traces of the gut, indicating that carcasses, and not molts, dominate. The preservation of soft and lightly sclerotized tissues indicates that soft-bodied fossils are rare due to unfavorable living conditions rather than loss through decay (Pari et al., 2021).

The preservation of highly labile tissues, such as the myomeres and eyes of chordates, in a relatively low-diversity soft-bodied assemblage in which fossils are not abundant, is an aspect of the Parker Quarry Lagerstätte that appears to be unique among Burgess Shale-type deposits. Preservation of such tissues generally occurs in association with a high abundance of soft-bodied fossils and with the highest diversity assemblages (Tier 1 of Gaines, 2014), and has been interpreted to reflect settings

where biostratinomic and diagenetic conditions for Burgess Shale-type preservation were optimized.

In many typical lower-diversity Burgess Shale-type assemblages, fossils were conserved under conditions that were persistently anoxic, yet in locations far enough from habitable benthic environments to render transportation to the preservation environment unlikely under low-energy depositional regimes dominated by claystone sediments (Gaines and Droser, 2010; Gaines, 2014). A notable aspect of the sedimentology of the Parker Quarry Lagerstätte, however, is the interbedding of sandstone and siltstone, and the presence of graded beds capped by massive claystones, indicating episodes of energetic deposition (Pari et al., 2021), in contrast to many outer-shelf Burgess Shale-type deposits, where mm-laminated claystones dominate (Gaines, 2014). The fine-grained fossil-bearing claystones are interpreted as the distal expression of energetic flows, which had sufficient power to transport organisms across chemical gradients (Pari et al., 2021); experimental studies have shown that delicate soft-bodied organisms can withstand significant transport (Allison, 1986; Bath Enright et al., 2021). The preservation of trilobite molt associations, however, suggests that trilobites intermittently colonized the seafloor locally (Whittington, 1988; Webster, 2009), although the activity of infaunal organisms was consistently excluded. The setting of the Parker Quarry Lagerstätte near the toe of a substantial break in depositional slope (Landing, 2007; Webster and Landing, 2016), as in the case of the Burgess Shale, appears to have been the key in promoting energetic conditions that resulted in the transport and burial of soft-bodied fossils, and ultimately, the remarkable preservation of labile tissues within many specimens.

Taphonomy

The major challenge to understanding the mode of preservation of soft-bodied fossils in the Parker Quarry Lagerstätte is weathering of the surfaces along which soft-bodied fossils occur. At Parker's Cobble, the interbedded mudstones exhibit a strong slaty cleavage that is parallel to bedding and therefore favorable for fossil quarrying (Pari et al., 2021), but also provides pathways for groundwater flow through the rock. A major consequence of this fluid flow is the oxidation of a portion of a substantial pyrite component of the slate, and Fe-oxide staining of surfaces and features of individual fossils (e.g., Figs. 2.2, 6, 10.5; Pari et al., 2021). Optical microscopy and elemental mapping also indicate that native S is present as veneers on some surfaces. Although S may be present in excess of Fe, optical microscopy and bulk chemical analyses (Pari et al., 2021) indicate that both are derived from oxidation of pyrite and redistribution across joints and fractures during recent oxidative weathering. Nevertheless, several fossils occur on relatively fresh, although not pristine, surfaces. These were selected for elemental mapping (see Material and methods).

Soft-bodied fossils of Burgess Shale-type are preserved as carbonaceous compressions, with anatomical features of some taxa replicated in calcium phosphate or pyrite (Butterfield, 2002; Gabbott et al., 2004; Gaines et al., 2008; Edgecombe et al., 2015), although debate has persisted regarding the role of pyrite and aluminosilicate-like minerals as pervasive mineral phases that capture soft-bodied anatomy (Orr et al., 1998;
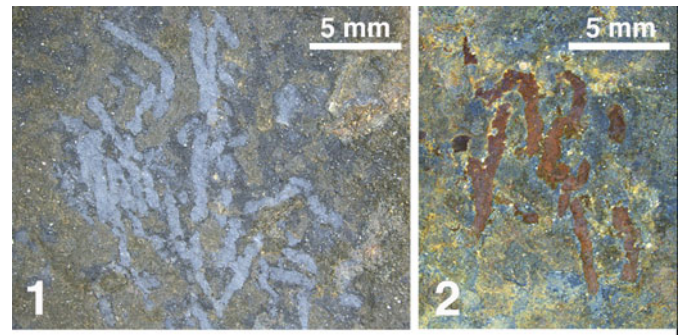

Figure 2. *Fuxianospira gyrata* Chen and Zhou, 1997. (**1**) YPM IP 239095. (**2**) YPM IP 239097.

Butterfield et al., 2007; Gaines, 2014; Schiffbauer et al., 2014; Broce and Schiffbauer, 2017; Anderson et al., 2021). The two soft-bodied fossils that were mapped here (Fig. 1), a possible priapulid (?*Ottoia*) (Fig. 4.1) and the new bivalved arthropod *Vermontcaris montcalmi* n. gen. n. sp. (Fig. 9.9), which occur in close proximity on the same bedding plane (Fig. 1.1, Pari et al., 2021, fig. 2G), provide evidence of the nature of soft-bodied preservation within the Parker Quarry Lagerstätte.

In the ?priapulid map (Fig. 1.1, area 2, 1.2), C picks out areas of the fossil that appear reflective to the naked eye. Carbon is most enriched in the structure interpreted as the gut, but also highlights cuticular annulations. The absence of Ca indicates that C within the fossil is organic in origin and not a constituent of a carbonate mineral. The distributions of Si, Al, and O, the core constituents of clay minerals, are essentially the inverse of C. Silicon is elevated on parts of the gut, but otherwise there is a consistently stronger signal of Si, O, and Al in the matrix than within the fossil. The distributions of K and Mg are similar to those of Si, O, and Al, but the signal of these two elements is significantly weaker.

Mapping of *V. montcalmi* n. gen. n. sp. (Fig. 1.1, area 3, 1.3) revealed elemental distributions similar to the ?priapulid. Areas of *V. montcalmi* n. gen. n. sp. that appear reflective to the naked eye are characterized by enrichment in C, and depleted in the matrix-forming elements Al, Si, and O. The inverse relationship of C versus Al, Si, and O in both fossils suggests that the range of elemental variation is largely controlled by variability in the thickness of the carbonaceous material that comprises them, which determines the degree to which the EDS signal of elements within the matrix is suppressed. Although C is particularly enriched in areas of both fossils, most regions of the fossils show no compositional difference to the matrix, a finding that has been interpreted for Burgess Shale-type fossils to represent the presence of vanishingly thin carbonaceous films with a C concentration below the detection limits of EDS (Gabbott et al., 2004; Gaines et al., 2008).

Sulfur picks out the entire cuticle of the ?priapulid more clearly than any other element. The distribution of Fe is similar, but its signal is much weaker and exhibits a clear inverse relationship with C. The distribution of S also corresponds well to the overall morphology of *Vermontcaris* n. gen., in contrast to the distribution of Fe in this specimen. Although correspondence of Fe and S can indicate the presence of pyrite, no crystals of pyrite are evident in either fossil under microscopy. EDS

spectra of the ?priapulid suggest that S is >4 times as abundant as Fe, whereas the expected S to Fe ratio in pyrite is 2:1. Iron is less conspicuous in *V. montcalmi* n. gen. n. sp. and shows weaker correspondence with S. The correspondence of Fe and O suggests that Fe is present in both fossils as an oxide, whereas the distribution of S suggests that it is in elemental form. The reddish hue of Fe-rich areas also suggests that Fe is present as an oxide rather than a sulfide phase. The most parsimonious interpretation, in the absence of evidence for pyrite crystals, is that both Fe and S represent secondary veneers over the cuticle that were derived from the weathering of pyrite in the bulk rock. Neither Fe nor S are enriched in bulk rock relative to composite shale standards (Pari et al., 2021).

Most specimens of *V. montcalmi* n. gen. n. sp. exhibit 3-dimensional preservation of the gut (Figs. 7–9). EDS spot analyses and elemental mapping confirm that the gut filling is comprised of matrix sediment, rather than an authigenic mineral such as calcium phosphate, which is a relatively common replacement in Burgess Shale-type (BST) fossils that captures anatomical information in arthropod guts and other soft-tissue features (Butterfield, 2002; Gaines et al., 2008; Aria et al., 2015; Nanglu and Caron, 2018). Three-dimensional preservation of the gut by sediment filling is conspicuously different from most BST fossils, but is prominent in some Chengjiang arthropods (Hou et al., 2017). It may reflect ingestion of sediment during turbid transport or deposit feeding.

In summary, data from elemental mapping support carbonaceous compressions as the primary mode of preservation of the soft-bodied fossils of the Parker Quarry Lagerstätte. Although pyrite is abundant within the sediments (Pari et al., 2021), it was rarely found in association with soft-bodied fossils (the specimen of the sponge illustrated in Fig. 3.4 is an exception). Authigenic clays or aluminosilicate-like minerals are also absent from the soft-bodied fossils. The formation of clay minerals during BST fossilization has been interpreted as a product of early diagenesis (Anderson et al., 2021) or metamorphism (Butterfield et al., 2007). In the latter case, authigenic clay minerals would be expected to have formed within the Parker Quarry Lagerstätte soft-bodied fossils as carbonaceous materials were volatilized during slate grade metamorphism. The unusual nature of the fossils from the Burgess Shale in British Columbia may reflect the alteration of most early diagenetic clay during the higher, greenschist grade of metamorphism experienced by that unit (Anderson et al., 2021).

Material and methods

Two trenches exposing surface areas of $\sim$50 m^2 and 25 m^2 were excavated to depths of up to 3 m using hand tools on the southwest flank of Parker's Cobble. Both trenches yielded soft-bodied fossils, at a combined rate of 0.7 specimens per m^3 (exclusive of algae). The new specimens were collected by GP between 2016 and 2019, except for a very few collected under his direction, by splitting large slabs of slate (Pari et al., 2021).

The elemental maps (Fig. 1) were generated with an EDS X-ray detector on an environmental scanning microscope (FEI Quanta 200 FEG) at the University of Windsor Great Lakes Institute for Environmental Research (Canada). The maps were run at 12 kV, spot size 5, map resolution 512 × 400 pixels,

dwell time 200 μs; each field of view (1.93 mm wide) was scanned eight times, and the data collated. In the case of the possible priapulid (YPM IP 239053), there were 228 fields of view and the map ran for 25 hours, 7 minutes; in the case of *Vermontcaris montcalmi* n. gen. n. sp. (YPM IP 543321), there were 192 fields of view and the map ran for 21 hours, 10 minutes. In addition, we conducted elemental mapping and spot analyses of several other specimens described herein using a Hitachi SU7000 at Yale, operated at 15 kv in VP mode at 100 pascals.

Repositories and institutional abbreviations.—Smithsonian Institution (USNM); Yale Peabody Museum of Natural History (YPM).

Systematic paleontology

?Division Chlorophyta
Genus *Fuxianospira* Chen and Zhou, 1997

Type species.—*Fuxianospira gyrata* Chen and Zhou, 1997, from the Yuanshan Formation, Chengjiang, Yunnan, China, by monotypy.

Fuxianospira gyrata Chen and Zhou, 1997
Figure 2

2021 *Fuxianospira gyrata* Chen and Zhou, 1997; Wang et al., 2021, p. 3, figs. 4–6 (includes a synonymy).

Holotype.—Early Life Research Center, Chengjiang ELRC80001, Yuanshan Formation, Chengjiang, Yunnan, China (Chen and Zhou, 1997, p. 88, fig. 143).

Description.—Masses of fragments of poorly preserved, carbonaceous strap-like features are preserved as reflective films (Fig. 2.1) or, in some cases, with a covering of iron oxide, presumably the result of weathering pyrite (Fig. 2.2). The straps are mainly straight, but many show curvature and folding, and they occasionally appear to branch. They are parallel sided, $\sim$0.5–1.0 mm wide, with irregular undulating margins and convex terminations. They rarely exceed 2 cm in length. No structure is evident on the cuticle.

Material.—YPM IP 239095, part and counterpart; YPM IP 239097.

Discussion.—The specimens fall into Morphogroup 1 of LoDuca et al. (2017) among early Paleozoic non-calcified macroalgae, and their morphology is consistent with that of *Fuxianospira*, which is common in the Chengjiang biota (LoDuca et al., 2015b, 2017; Wang et al., 2021). The undulating margins reflect the coiled structure, although the preservation, like that of occurrences of *Fuxianospora* elsewhere (LoDuca et al., 2015b; Wang et al., 2021), is inadequate to show the morphology in detail. The apparent branching is likely the result of overlap (see LoDuca et al., 2015b, fig. 1). The thalli of *Sinocylindra*, which is also from the Chengjiang biota, tend to be longer and thinner, with smoother margins (Wang et al., 2021). We follow LoDuca

et al. (2015b) and Wang et al. (2021) in tentatively assigning *Fuxianospira* to Chlorophyta.

Remarks.—Similar specimens from other Cambrian localities were assigned mainly to *Yuknessia simplex* Walcott, 1919, which was originally described from the Burgess Shale and interpreted by Walcott (1919) as an alga. LoDuca et al. (2015a) showed that most of Walcott's Burgess Shale specimens preserve banding on the cuticle and identified them as a benthic colonial pterobranch hemichordate (see also Ramírez-Guerrero and Cameron, 2021); just a few of Walcott's specimens turned out to be algal. However, LoDuca et al. (2015b) also investigated specimens attributed to *Yuknessia* from the Chengjiang biota in China and other Cambrian Lagerstätten in North America, and assigned them to the alga *Fuxianospora* Chen and Zhou, 1997.

Phylum Porifera Grant, 1836
Class Ascospongiae Botting, 2021
Family Leptomitidae de Laubenfels, 1955
Genus *Leptomitus* Walcott, 1886

Type species.—*Leptomitus zitteli* Walcott, 1886, Parker Formation, Parker Quarry, Franklin County, Vermont, USA.

Leptomitus zitteli Walcott, 1886
Figure 3.1–3.7

1987 *Leptomitus zitteli* Walcott, 1886; Rigby, p. 453, fig. 3.3–3.5 (includes a synonymy).
2021 *Leptomitus*; Pari et al., p. 693, fig. 2I.

Lectotype.—USNM 15308, Parker Formation, Parker Quarry, Franklin County, Vermont, USA. Cambrian Series 2, Stage 4 (Rigby, 1987, fig. 3.3–3.5).

Occurrence.—*Leptomitus zitteli* is presently known only from the Parker Formation at Parker's Cobble (Rigby, 1987; García-Bellido et al., 2007).

Description.—Rigby (1987) described the spicular structure of this elongate tubular sponge, which comprises an outer layer of parallel oxeas and an inner layer of tiny horizontal spicules (Fig. 3.1, 3.3). The lectotype (USNM 15308) reveals a plumose arrangement of spicules at the distal end (Fig. 3.2), which may represent their arrangement in the interior of the skeleton (Rigby, 1987). It is difficult to distinguish between coarse and fine long vertical oxeas and to determine their length. Dimensions of the sponge vary between specimens. YPM IP 543326 is a fragment ~70 mm long consisting of a bundle of oxeas, roughly aligned, with some diverging at either end (Fig. 3.4). The specimen is preserved in pyrite, which prevents individual spicules from being distinguished. USNM 15308, which is ~70 mm long, varies in width from 10–2 mm along its length. YPM IP 239151 (Fig. 3.5–3.7) is longer than other specimens from this locality at 12 cm, although incompletely exposed, but only 2–4 mm wide along its length. The distribution of the spicules indicates some decay and exfoliation along its length with small fragments

displaced laterally and evidence that the outer layer has separated at one point about halfway along the preserved length, giving the appearance of branching. This is consistent with the occurrence of sponge fragments such as YPM IP 543326 (Fig. 3.4) and YPM IP 239096.

Material.—USNM 15308, lectotype, and USNM 419730 and 419732 on the same block, part and counterpart. USNM 419731, part and counterpart, on a different block, YPM IP 239096, YPM IP 239151, YPM IP 239152, YPM IP 543326.

Remarks.—Rigby (1986) published a generalized reconstruction of *Leptomitus* based on his revision of *L. lineatus* (Walcott, 1920) from the Burgess Shale. The following year he provided a full description of Walcott's material of *L. zitteli*, and a synonymy (Rigby, 1987). He designated as lectotype the best-preserved specimen, USNM 15308, part and counterpart, which Walcott (1886, legend to plate 2) referred to as the type specimen (the other two specimens on the same block now carry the numbers USNM 419730 and 419732). A specimen on a second block and two non-contiguous fragments of its counterpart were also originally included under USNM 15308, but that individual is now numbered USNM 419731.

Class Hexactinellida Schmidt, 1870
Order Reticulosa Reid, 1958
Superfamily Protospongioidea Finks, 1960
Family Protospongiidae Hinde, 1887
Genus ?*Protospongia* Salter, 1864

Type species.—*Protospongia fenestrata* Salter, 1864, Menevian Group, Porthyrhaw, St. Davids, Wales.

?*Protospongia hicksi* Hinde, 1887
Figure 3.8, 3.9

1987 ?*Protospongia hicksi* Hinde, 1887; Rigby, p. 459, fig. 4.

Holotype.—Sedgwick Museum, Cambridge SM A1035, Menevian Group, Porthyrhaw, St. Davids, Wales.

Occurrence.—In addition to this probable occurrence in the Parker Formation at Parker's Cobble (Rigby, 1987), *Protospongia hicksi* is present in younger North American Cambrian Lagerstätten, including the Burgess Shale (Rigby, 1986) and the Trilobite Beds on Mount Stephen (Rigby and Collins, 2004). Spicules closely resembling those of *Protospongia* also have been reported from the upper part of the Kinzers Formation near Lancaster, Pennsylvania, which is similar in age to the Mount Stephen Trilobite Beds (Campbell, 1971).

Material.—Fragments and isolated spicules associated with USNM 15308, USNM 419731, and USNM 419732.

Remarks.—We follow Rigby (1987) in tentatively assigning these spicules to ?*Protospongia hicksi*. In doing so, however, we acknowledge that their morphology is poorly constrained.
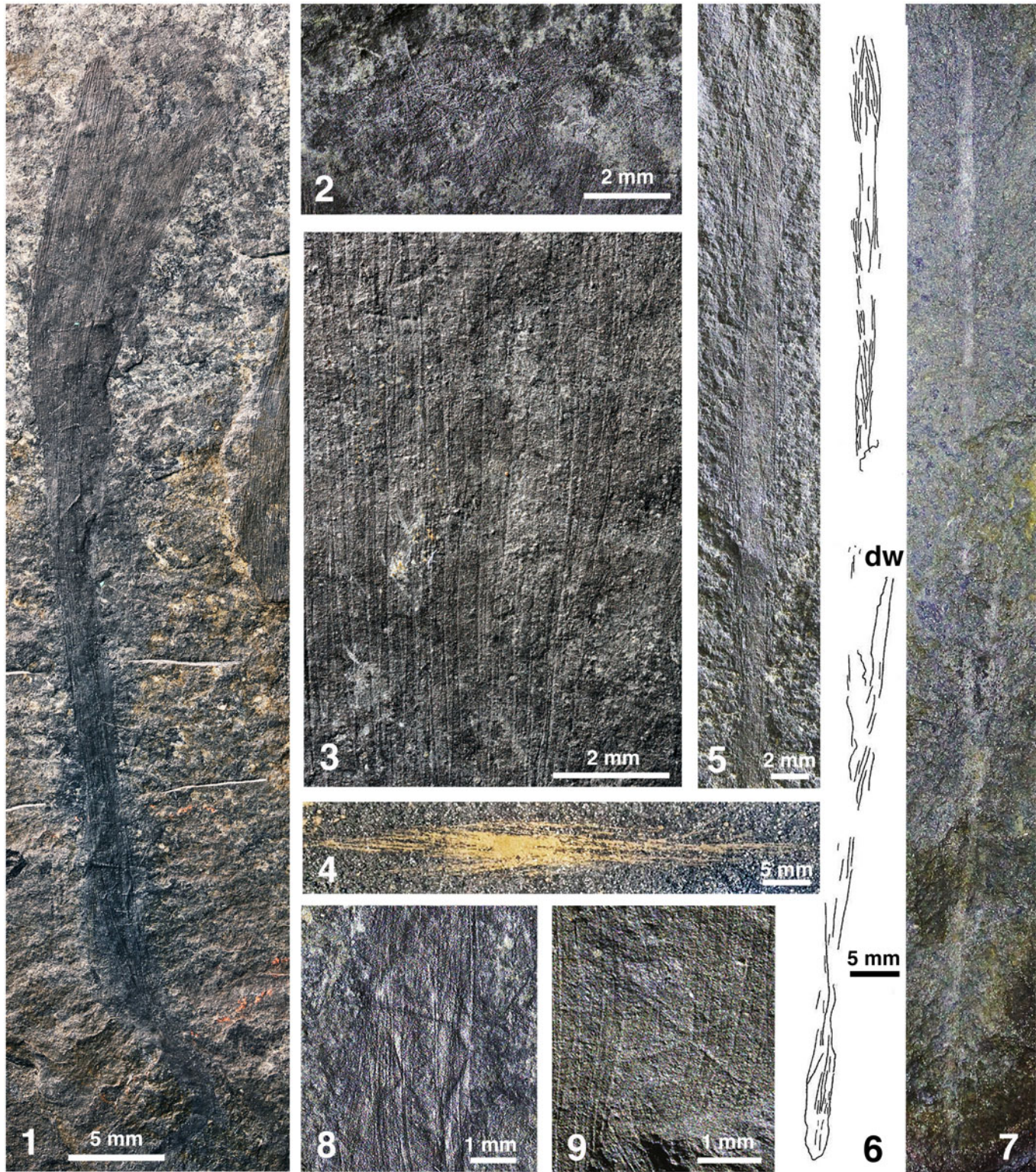
Figure 3. (**1–7**) *Leptomitus zitteli* Walcott, 1886. (**1–3**) USNM 15308, lectotype, entire specimen, plumose spicules evident at distal termination, long vertical and short horizontal oxeas. (**4**) YPM IP 543326, isolated bunch of oxeas. (**5–7**) YPM IP 239151, distal end showing long vertical oxeas, explanatory drawing of entire specimen (dw = detached wall), and entire specimen showing apparent branching. (**8, 9**) ?*Protospongia hicksi* Hinde, 1887, isolated cruciform spicules associated with USNM 15308, and associated with USNM 419731.

Protospongia and similar taxa are in need of revision (Botting and Muir, 2018) and may be more appropriately assigned to Ascospongiae than to Hexactinellida (Botting, 2021). Rigby

(1987) recorded ?*Protospongia hicksi* in intimate association with the specimens of *L. zitteli* on the slab that includes the lectotype USNM 15308. Rigby (1987, p. 459) noted that the

lectotype, in its middle part, appears to have "buried a partially intact fragment of a protosponge" and (1987, p. 460) "isolated *Protospongia*-like stauracts occur scattered throughout matrix between *Leptomitus* fragments." He also observed first order quadrules associated with USNM 419732. These *Protospongia* spicules were not noted by Walcott (1886). We illustrate examples of these cruciform spicules from Walcott's original specimens here (Fig. 3.8, 3.9). We did not find examples associated with the specimens of *Leptomitus* discovered during our excavations.

Superphylum Ecdysozoa Aguinaldo et al., 1997
Phylum ?Priapulida Delage and Hérouard, 1897, stem group
Class uncertain
Order uncertain
Family ?Ottoiidae Walcott, 1911
Genus ?*Ottoia* Walcott, 1911

Type species.—Ottoia prolifica Walcott, 1911 (Walcott, 1911b), Burgess Shale, British Columbia, Canada.

?*Ottoia* sp.
Figure 4

2021   Priapulid reminiscent of *Ottoia*; Pari et al., p. 695, fig. 2G.

Description.—The specimen, YPM IP 239053, which is ~9.5 cm long, with a maximum width of 8.5–9 mm, is tightly coiled (Fig. 4). It narrows gradually toward one end, curving sharply and expanding slightly at the termination, resulting in an outline reminiscent of a proboscis. The other end tapers more abruptly. Details are poorly preserved, but the body preserves evidence of transverse annulations and a wide reflective structure in the anterior portion that may represent the gut.

Material.—YPM IP 239053.

Remarks.—The annulations and presumed proboscis suggest a priapulid affinity, and the outline of the specimen is similar to *Ottoia*, among Cambrian genera. Smith et al. (2015) demonstrated the value of sclerites in distinguishing species of ottoiids and they cautioned against identifying indeterminate priapulids that do not preserve such characters. On this basis, we assign our specimen to *Ottoia* with a query. Smith et al. (2015, p. 706) noted that "there are no confirmed records of *Ottoia* macrofossils outside the Burgess Shale," but Y. Yang et al. (2016) described a new species based on multiple body fossils from the Kaili Formation in South China, demonstrating the occurrence of the genus outside Laurentia. Resser and Howell (1938, p. 215) tentatively assigned a specimen from the Kinzers Formation to *Ottoia*, but Conway Morris (1977, p. 85) identified it as a palaeoscolecid. If the Parker Formation specimen were *Ottoia*, it would be the oldest macrofossil representative of the genus discovered to date. Sansom (2016) noted the decay-resistant nature of sclerites in living priapulids, and Howard et al. (2020) indicated that their absence is a feature of stem ecdysozoans. YPM IP 239053 preserves cuticle annulations in
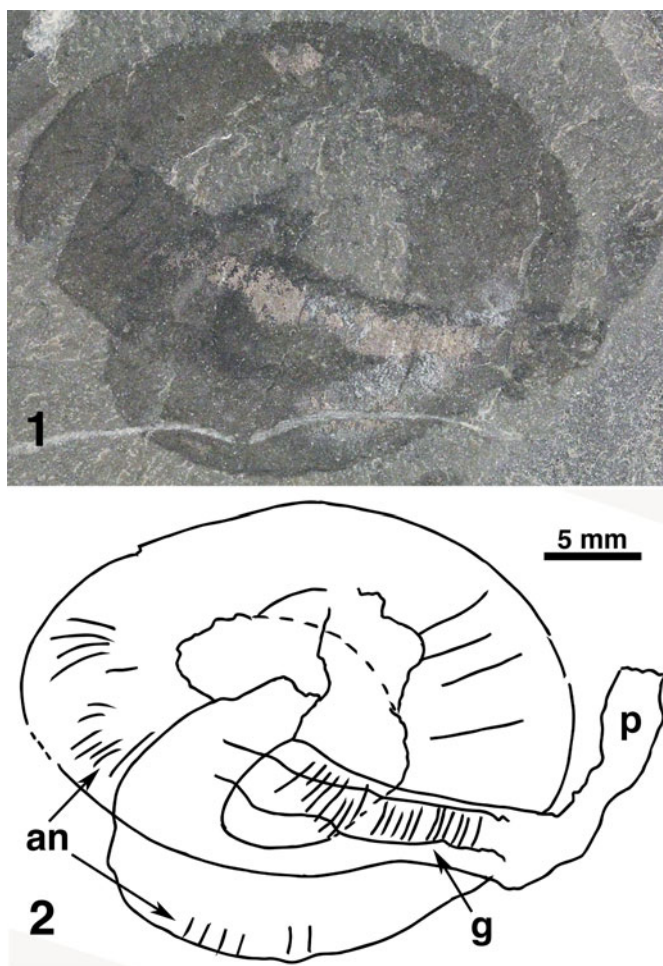

Figure 4.   ?*Ottoia* Walcott, 1911 (Walcott, 1911b), (**1, 2**) YPM IP 239053, specimen and explanatory drawing. an = trunk annulations; g = gut trace; p = proboscis.

places, but the distribution of carbon on the specimen and the associated *Vermontcaris montcalmi* n. gen. n. sp., is patchy (fig. 1), presumably as a result of degradation. Thus the apparent absence of scalids on the presumed proboscis may or may not be real (Howard et al., 2020). Thus the fossil may represent a stem ecdysozoan similar to *Acosmia maotiania* Chen and Zhou, 1997, rather than a stem priapulid.

The specimen shows some similarity to *Atalotaenia adela* García-Bellido and Conway Morris, 1999, from the Kinzers Formation (García-Bellido and Conway Morris, 1999). However, the single reported specimen of *A. adela* is incomplete, it preserves a ribbon-like structure for which there is no equivalent in YPM IP 239053, and the annulations are more widely separated. García-Bellido and Conway Morris (1999) assigned *A. adela* to Phylum, Class, Family uncertain.

Panarthropoda Nielsen, 1995
Order Radiodonta Collins, 1996
Family Amplectobeluidae Pates et al., 2021
Amplectobeluidae indet.
Figure 5
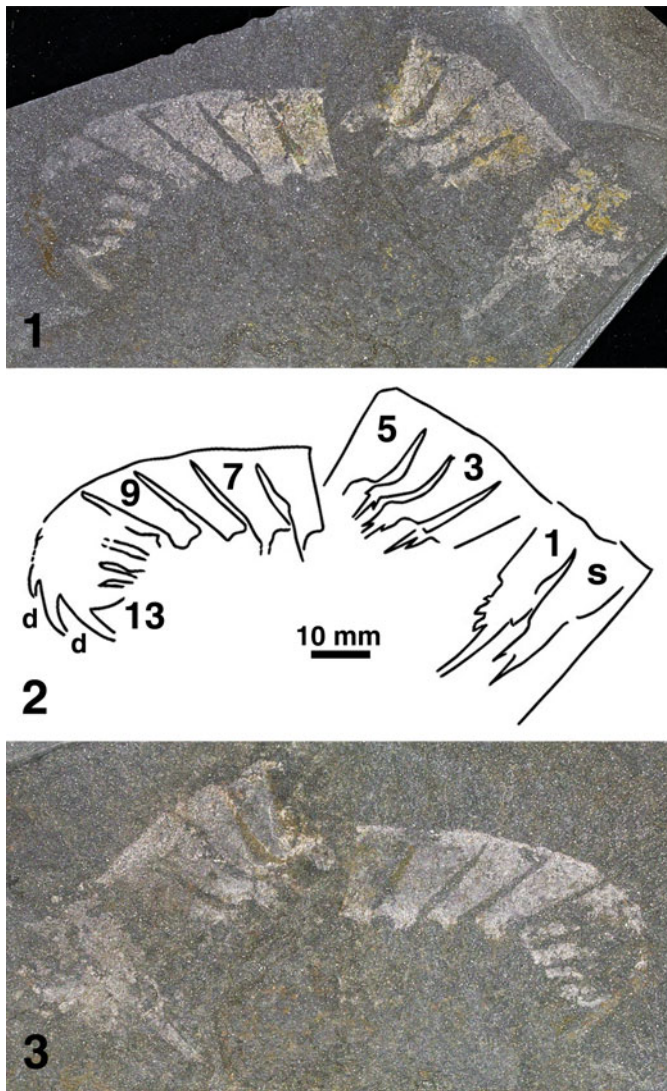
2021   Radiodont; Pari et al., p. 695, fig. 2F.

Figure 5. Radiodont appendage. (**1–3**) YPM IP 239052, part, explanatory drawing, and counterpart. d = dorsal spine; s = distalmost podomere of shaft; 1, 3, 5, etc. = podomeres of articulated region.

Description.—The specimen, which is preserved in lateral view, is comprised of the distalmost podomere of the shaft, which bears a large endite (= ventral spine: see Guo et al., 2019), and an articulated region of 13 podomeres, each bearing ventrally projecting endites with short lateral auxiliary spines (Fig. 5). The proximal part of the shaft and the endites, particularly in the more distal part of the appendage, are incomplete, which limits the detail available. Decay and disarticulation have resulted in separation of the appendage into two portions at the junction between podomeres 5 and 6 in the distal articulated region; the junction between podomeres 1 and 2 is also partially ruptured. Podomeres 6–9 of the articulated region are a little longer than those proximal to them, and the height (measured from the mid-point of the dorsal margin to apparent attachment of the endite) to length ratio of the podomeres averages ~2.0. It is not clear whether the endites are paired or not. The podomeres are separated by a gap,

tapering dorsally, which represents the position of the articulating membrane. In spite of poor preservation it is clear that the endite on the distalmost podomere of the shaft and on the first podomere of the articulated region are enlarged (hypertrophied) compared to the rest (Fig. 5). The endite on podomere 1 of the articulated region is the largest, and three auxiliary spines radiate from its distal margin. The endite on podomere 2 is shorter than that on podomere 3. The endite on podomere 5 appears enlarged and was presumably longer than on podomere 3, based on the width at its base. Long robust dorsal spines are present on the distalmost podomeres, which curve strongly ventrally, and the thirteenth podomere bears two terminal spines. The specimen measures ~140 mm along its dorsal margin excluding the dorsal spines on the distal segments and the gap resulting from disarticulation.

Material.—YPM IP 239052, part and counterpart.

Discussion.—This specimen represents the first record of a radiodont from the Parker Formation and adds a new locality for this group on the Laurentian paleocontinent (Pates and Daley, 2019).

Remarks.—Although radiodont families are diagnosed on the basis of the complete morphology of the animal, and the mouth parts are particularly characteristic (Cong et al., 2018), specimens are often assigned, even to species, based on the frontal appendages (Pates et al., 2021). As far as can be determined, the morphology of the Parker Formation appendage does not correspond precisely to that of any previously described radiodont (see Cong et al., 2018; Guo et al., 2019; Pates and Daley, 2019; Pates et al., 2021). It is incomplete proximally but likely comprises the distalmost podomere of the shaft, which bears a large hypertrophied endite, and an articulated region of 13 podomeres. It shows greatest similarity to Anomalocarididae and Amplectobeluidae, both of which include genera with paired endites. YPM IP 239052 differs from Anomalocarididae in the relative lengths of the endites and details of the auxiliary spines (Guo et al., 2019; Pates and Daley, 2019; Pates et al., 2021). It shows greater similarity to the frontal appendage of Amplectobeluidae, which has a single hypertrophied proximal endite on the first podomere of the articulated portion, high/deep podomeres 12 or 13 in number, robust dorsal spines on the distalmost podomeres, and an endite on podomere 5 of the articulated region that is enlarged relative to that on podomere 3 (Cong et al., 2018; Guo et al., 2019; Pates et al., 2021). This last character is particularly evident in *Ramskoeldia* from the Chengjiang biota of China (Series 2, Stage 3), but that genus lacks a large endite on the shaft (Pates et al., 2021). The large height to length ratio of the podomeres, large first endite on the articulated region, and pronounced distal dorsal spines are shared with *Amplectobelua* (Daley and Budd, 2010; Lerosey-Aubril et al., 2020), but the articulated region of the Parker Formation appendage includes 13 as opposed to 12 podomeres. The Parker Formation appendage shares more characters with *Laminacaris chimera* Guo et al., 2019, from the Chengjiang biota than with *Amplectobelua*, including a large endite on the shaft, 13 podomeres in the articulated region, and a

larger endite on podomere 5 of that region than podomere 3 (Guo et al., 2019). *Laminacaris* has been recovered as an amplectobeluid in some phylogenetic analyses (Lerosey-Aubril and Pates, 2018; but see Moysiuk and Caron, 2021).

The phylogeny of radiodonts is not well resolved, but Anomalocarididae and Amplectobeluidae fall within the same clade (Cong et al., 2014; Vinther et al., 2014; Van Roy et al., 2015; Lerosey-Aubril and Pates, 2018; Moysiuk and Caron, 2021). The available evidence supports assignment of the Parker appendage to Amplectobeluidae. It shows similarities to a number of genera, but we do not assign it beyond family here in view of the incomplete preservation. The Parker Formation appendage may represent a new genus and species within this group.

Class uncertain
Order Tuzoida Simonetta and Delle Cave, 1975
Family Tuzoiidae Raymond, 1935
Genus *Tuzoia* Walcott, 1912

Type species.—*Tuzoia retifera* Walcott, 1912 (Walcott, 1912a), Burgess Shale, British Columbia, Canada.

Tuzoia polleni Resser, 1929
Figure 6.1–6.10

1890 Problematical organic marking; Walcott, pl. 59, fig. 1.
1938 *Tuzoia vermontensis* Resser and Howell, p. 231, pl. 13, fig. 1.
2003 *Tuzoia polleni* Resser, 1929; Lieberman, p. 681.
2007 *Tuzoia polleni* Resser, 1929; Vannier et al., p. 460, fig. 17.2, p. 462 (includes a synonymy).
2021 *Tuzoia polleni* Resser, 1929; Pari et al., p. 694, fig. 2B, C.

Holotype.—USNM 80485, Eager Formation, Cranbrook, British Columbia, Canada (Resser, 1929, pl. 5, fig. 1).

Description.—USNM 26728 (Fig. 6.1, 6.2) represents a single right valve with an unusual subcircular outline. It preserves four spines on the posterior margin and perhaps five along the hinge line (only the posteriormost of these five is clearly preserved, the others are somewhat equivocal and have been outlined in pencil on the specimen). YPM IP 239051 (Fig. 6.3, 6.4) and YPM IP 239150 (Fig. 6.5, 6.6) also reveal the complete valve outline. The ventral margin of most of the specimens is followed by a well-delineated wide margin (Fig. 6.3–6.8), which may be modified by compression. YPM IP 239051 (Fig. 6.3, 6.4) preserves at least four spines around the posterior margin. There is also at least one spine on the anterior margin and there may be several on the hinge line, but these cannot be discerned with confidence due to the nature of the preservation. YPM IP 239150 (Fig. 6.5, 6.6), which preserves both valves slightly offset, preserves two slender posterior spines on each valve. YPM IP 239149 (Fig. 6.7, 6.8) and YPM IP 543331 (Fig. 6.9, 6.10) are incompletely exposed. They preserve four and seven spines, respectively, around the posterior margin; in neither case are spines evident on the hinge. Most of the specimens preserve a trace of the lateral ridge (Fig. 6.1–6.4, 6.7, 6.8) roughly aligned with the mid-posterior spine, its position and shape

varying with the orientation and flattening of the carapace. Spines are not evident along the ridge, but these are difficult to discern when flattened onto the valve.

USNM 26728 (Fig. 6.1, 6.2) is 8 cm long and 7.6 cm high excluding spines (height/length, H/L 0.95). YPM IP 239051 (Fig. 6.3, 6.4) is 7.4 cm long and 4.7 cm high (H/L 0.64). YPM IP 239149 (Fig. 6.7, 6.8) and YPM IP 543331 (Fig. 6.9, 6.10) are ~3.9 cm high and ~6.2 cm high, respectively, based on extrapolations from the exposed parts of the valves. YPM IP 239150 (Fig. 6.5, 6.6) preserves both valves offset; the completely exposed (?left) valve is ~4.8 cm long and 3.2 cm high (H/L 0.67).

Material.—USNM 26728, the only previously known specimen of *Tuzoia* from this locality, and four new specimens with part and counterpart: YPM IP 543331, YPM IP 239051, YPM IP 239149, YPM IP 239150.

Discussion.—The wide ventral margin in the new specimens from the Parker Quarry Lagerstätte is similar to that in *Tuzoia* sp. from the Emu Bay Shale of Australia, which was interpreted as a doublure (García-Bellido et al., 2009). Variability in the preservation of the carapace outline and spines makes the identification of species of *Tuzoia* difficult (Vannier et al., 2007). The shape and number of spines may change during ontogeny (Wen et al., 2015). The number of spines evident around the margin of the valves also shows intraspecific variability, which may reflect morphologic differences and/or taphonomic processes (Liebermann, 2003; Vannier et al., 2007). USNM 26728 (Fig. 6.1, 6.2) shows a much greater height to length ratio than YPM IP 239051 (Fig. 6.3, 6.4) and YPM IP 239150 (Fig. 6.5, 6.6). This might be a result of burial of USNM 26728 with the valve tilted at an angle to bedding and consequent reduction of the length, but, apart from a hint of concentric lines close to the anterior margin of the valve, there is no independent evidence that this is the case. Specimens of the new arthropod *Vermontcaris montcalmi* n. gen. n. sp., however, clearly vary in outline as a consequence of flattening in different attitudes to bedding following transport and burial (Figs. 7–9). Such variation in orientation is analogous with that in the Burgess Shale and is consistent with evidence that the Parker Quarry Lagerstätte sediments were deposited from dense mud-rich flows (Pari et al., 2021). Carapaces of *Tuzoia* from other localities are also characterized by variation in outline (Vannier et al., 2007).

If the length of USNM 26728 (Fig. 6.1, 6.2) does reflect compaction at an angle to bedding, its original length can be estimated based on the height to length ratio of YPM IP 239051 (Fig. 6.3, 6.4), which would extend it from 8 cm to 11.9 cm. This exceeds the maximum length of ~10 cm reported for *T. polleni* by Vannier et al. (2007, p. 462). Valves of *Tuzoia* up to ~18 cm long have been reported from the Cambrian Miaolingian (Drumian) of Bohemia (Chlupáč and Kordule, 2002, fig. 3), but the largest North American examples previously noted, specimens of *T. retifera* from the Burgess Shale, reached maximum lengths of ~12 cm (Vannier et al., 2007).

Remarks.—Walcott (1890) figured USNM 26728 (Fig. 6.1, 6.2), without description, noting it as "a problematical organic
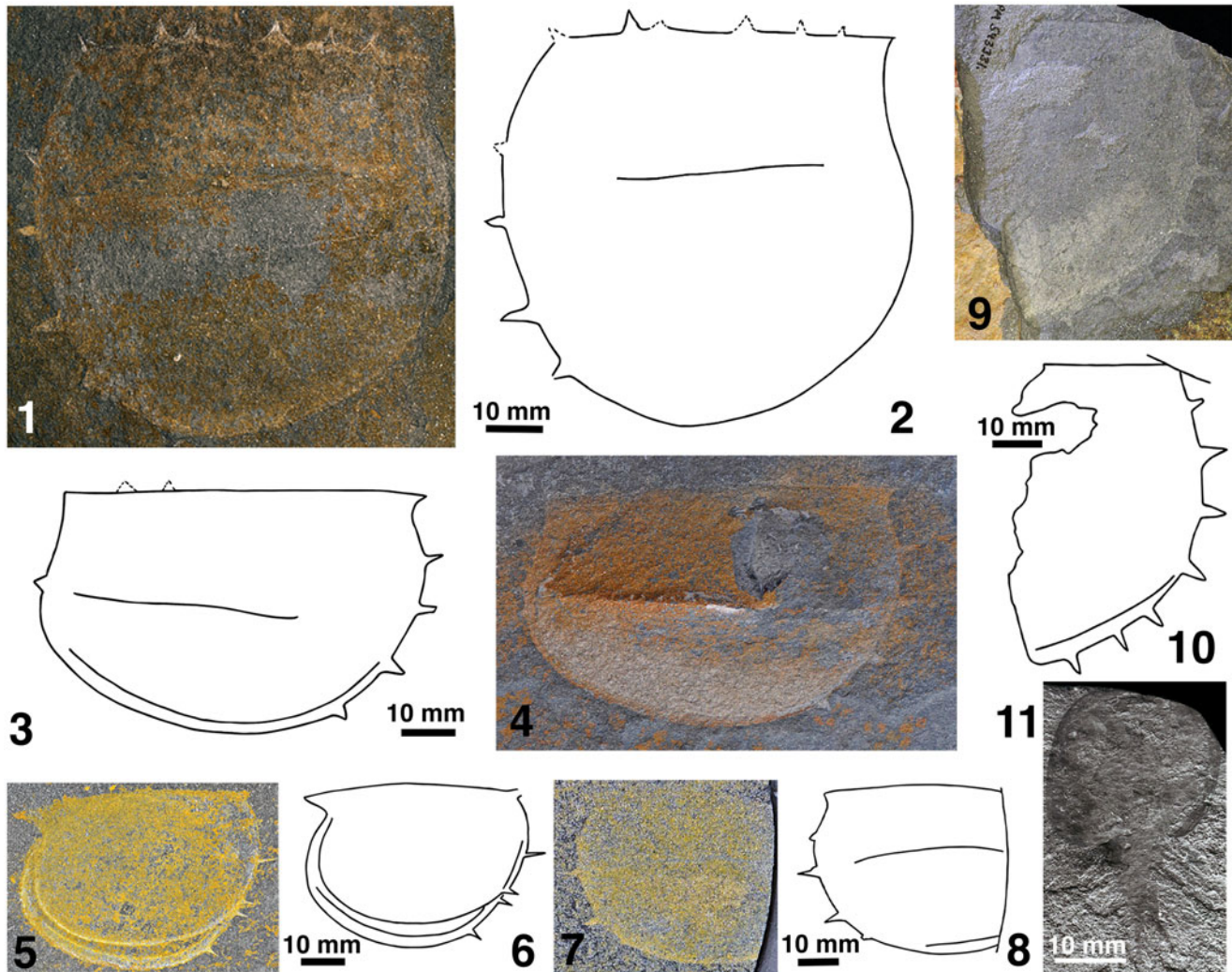
Figure 6. (**1–10**) *Tuzoia polleni* Resser, 1929. (**1, 2**) USNM 26728, specimen and explanatory drawing; (**3, 4**) YPM IP 239051, explanatory drawing and specimen; (**5, 6**) YPM IP 239150, specimen and explanatory drawing; (**7, 8**) YPM IP 239149, specimen and explanatory drawing; (**9, 10**) YPM IP 543331, specimen and explanatory drawing. (**11**) *Protocaris marshi* Walcott, 1884, USNM 15400, holotype.

marking," and the specimen was subsequently labeled as Medusa? sp. (Resser and Howell, 1938, p. 231). Resser and Howell (1938) described it as *Tuzoia vermontensis*, a new species of the genus that Walcott (1912a) had erected for Burgess Shale material. Lieberman (2003) synonymized all the species of *Tuzoia* (*T. polleni*, *T. nodosa* Resser, 1929, and *T. spinosa* Resser, 1929) that Resser (1929) originally described from the Eager Formation, assigning them to *T. polleni*. Lieberman (2003) did not examine the original specimen of *T. vermontensis*, USNM 26728, but interpreted it as a single valve and synonymized it with *T. polleni* because of the presence of spines on the entire margin. Vannier et al. (2007) went further and synonymized *T. nitida* Resser and Howell, 1938, from the Kinzers Formation with *T. polleni*. They tentatively retained *T. vermontensis* as a synonym of *T. polleni* (Vannier et al., 2007, p. 463), but they interpreted the spines along the dorsal margin (hinge line) as ridge spines on the right valve (Vannier et al., 2007, fig. 17.2) based on their erroneous interpretation of USNM 26728 as a dorsoventrally compacted ('butterflied') specimen showing both valves.

The Parker Quarry Lagerstätte specimens vary in outline and the distribution of spines (Fig. 6). Identification is compromised by the lack of a dorsoventrally flattened specimen, which might show spines on the lateral ridge; clear evidence of reticulation is also absent. The morphological features of the Parker Quarry Lagerstätte specimens show a general similarity to *T. canadensis* Resser, 1929, as well as to *T. polleni* (Pari et al., 2021; see Vannier et al., 2007, fig. 25.3, 25.5). We follow Lieberman (2003) and Vannier et al. (2007) in synonymizing the Parker Formation *T. vermontensis* with *T. polleni*. We note, however, that future discoveries and analysis may show otherwise, or even that the new specimens may represent a different species to Walcott's original, in which case more than one species is present in the Parker Formation, as in the Burgess Shale (Vannier et al., 2007) and the Balang Formation of Guizhou, China (Wen et al., 2019).

<div align="center">

Class uncertain
Family Protocarididae Miller, 1889
Genus *Protocaris* Walcott, 1884

</div>

Type species.—*Protocaris marshi* Walcott, 1884, Parker Formation, Parker Quarry, Franklin County, Vermont, USA.

Protocaris marshi Walcott, 1884
Figure 6.11

1976 *Protocaris marshi* Walcott, 1884; Briggs, p. 2, text figs. 1, 3, pl. 1, figs. 1–3 (includes a synonymy).
2008 *Protocaris marshi* Walcott, 1884; Budd, p. 567.
2021 *Protocaris marshi* Walcott, 1884; Pari et al., p. 693, fig. 2A.

Holotype and only known specimen.—USNM 15400, Parker Formation, Parker Quarry, Franklin County, Vermont, USA.

Discussion.—In the absence of additional specimens we cannot add to the description by Briggs (1976). *Protocaris marshi* is arguably the first soft-bodied Cambrian arthropod described in the literature (Walcott, 1884; see Pari et al., 2021). Simonetta and Delle Cave (1975) assigned *P. marshi* to a new Order Protocaridida, without a diagnosis. Budd (2008) noted the likely presence in *P. marshi* of an 'anterior sclerite' based on the illustrations in Briggs (1976), a feature that Budd identified in a diversity of early arthropods, but otherwise *P. marshi* has received relatively little attention. Legg et al. (2013, fig. 4b) placed it on the stem leading to Euarthropoda. Aria and Caron (2017) amended Protocarididae to include *Branchiocaris*, *Tokummia*, and *Loricicaris*, noting that the assignment of *Protocaris* to their newly diagnosed Protocarididae is provisional. Aria and Caron's (2017) new diagnosis of Protocarididae includes multiple appendage characters, which are not preserved in *Protocaris*. They assigned Protocarididae to an emended Order Hymenocarina and recovered them as stem mandibulates rather than on the stem of euarthropods.

Remarks.—USNM 15400 (Fig. 6.11; see Briggs, 1976, text fig. 3, pl. 1, figs. 1–3), the holotype and only known specimen, was redescribed by Briggs (1976) who provided a full synonymy. A specimen from the Kinzers Formation of Pennsylvania (USNM 90826, counterpart in the North Museum, Franklin and Marshall College, P-A-392) referred to this taxon by Resser and Howell (1938), was rejected as unidentifiable (Briggs, 1976).

Class uncertain
Order uncertain
Family uncertain
Genus *Vermontcaris* new genus

Type species.—*Vermontcaris montcalmi* n. gen. n. sp.

Diagnosis.—As for species.

Etymology.—After the State of Vermont in which the locality occurs, plus Latin *caris* for crab.

Remarks.—Walcott (1886) compared the specimens of this taxon available to him to graptolites, referring them to *Diplograptus*? *simplex* (see Conway Morris, 1993, for a

history of early research). Resser and Howell (1938) assigned the material to a new genus, *Emmonsaspis*, noting (p. 233) that "the central rod, the ribbing, and the general shape of this animal argue strongly for its reference to the chordates." Shaw (1955), in contrast, regarded the affinities of the animal as unknown. Conway Morris (1989, 1993) noted that most of the specimens are similar to the Burgess Shale bivalved arthropod *Perspicaris* Briggs, 1977. He realized that the central rod, presumably interpreted by Resser and Howell (1938) as a notochord, is the gut and he also observed evidence of a carapace and trunk, and occasional traces of appendages (Conway Morris, 1993). All but one of the specimens figured by Resser and Howell (1938, pl. 9, figs. 2–4) are examples of this arthropod (Fig. 7.1–7.6), which we assign, together with new material (Figs. 9, 10), to *Vermontcaris* n. gen. because they differ from previously described taxa. The other figured specimen (USNM 15314A: Resser and Howell, 1938, pl. 9, fig. 1) is the lectotype of the chordate *Emmonsaspis cambrensis* (Walcott, 1890) (Conway Morris, 1993; Conway Morris and Caron, 2014) (see Remarks on *Emmonsaspis cambrensis*).

Vermontcaris montcalmi new species
Figures 7–9

1886 *Diplograptus*? *simplex* Walcott, part, p. 92, pl. 11, fig. 4 (non fig. 4a).
1889 *Phyllograptus*? *simplex* Walcott, part, p. 388.
1890 *Phyllograptus*? *cambrensis* (Walcott), part, p. 604, pl. 59, fig. 3a (non fig. 3).
1938 *Emmonsaspis cambriensis* (Walcott); Resser and Howell, part, p. 233, pl. 9, figs. 2–4 (non fig. 1).
1989 Arthropod, ?comparable to *Perspicaris*; Conway Morris, p. 278.
1993 Arthropod, ?comparable to *Perspicaris*; Conway Morris, p. 600.
2021 New bivalved arthropod; Pari et al., p. 693, fig. 2D, G.

Holotype.—YPM IP 543320.

Diagnosis.—Carapace with hinge line, valves suboval, eyes pedunculate, borne on a projection of the cephalon, trunk divided into a thorax of up to 40 short segments, similar in length, bearing elongate biramous appendages, and an apodous abdomen of 4 or 5 longer segments increasing in length posteriorly. Short telson tapering to a point, flanked by leaf-like appendages borne by the posteriormost abdominal somite.

Description.—The head region is concealed by the carapace. Only a projection bearing the eyes extends beyond the valves. The eyes are borne on stalks attached a short distance from the end of this projection (Figs. 8.3, 8.4, 9.7, 9.8). They are suboval in outline, whether flattened parallel to bedding (Fig. 8.3, 8.4, where they are rotated relative to the carapace) or in lateral aspect (Figs. 8.5, 8.6, 8.8–8.10, 9.9, 9.10), indicating that they were ovoid in shape. None of the specimens preserves evidence of antenniform limbs. Small, poorly defined paired structures, one positive, the
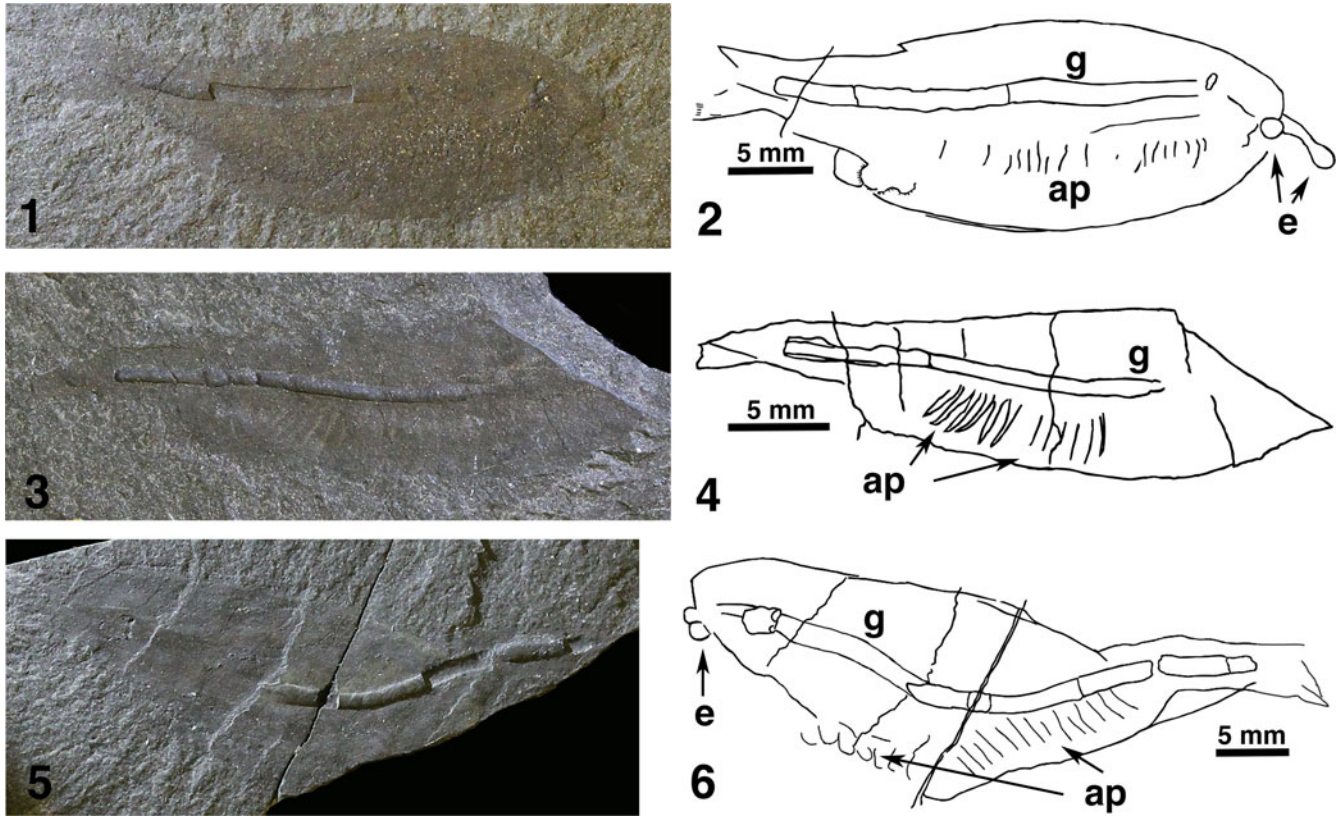
Figure 7. *Vermontcaris montcalmi* n. gen. n. sp. (**1, 2**) USNM 15314D, specimen and explanatory drawing. (**3, 4**) USNM 15314E, specimen and explanatory drawing. (**5, 6**) USNM 15314F, specimen and explanatory drawing. ap = thoracic appendages; e = eye; g = gut trace.

other negative in relief, are evident in the anterior part of the carapace of some specimens (Figs. 8.8–8.10, 9.1, 9.2); they may represent the impression of a more heavily cuticularized appendage, perhaps equipped for feeding. Specimens in which the carapace is flipped forward (Figs. 8.5, 8.6, 8.8–8.10, 9.5–9.10) indicate that it was only attached in the head region; no evidence of adductor muscle scars is preserved. The valves are elongate oval, but the preserved outline varies with attitude to bedding (compare Fig. 9.1, 9.2 with 9.3, 9.4).

The bivalved carapace covers most of the trunk, which is divided into two tagmata referred to here as thorax and abdomen. Only the posteriormost segments of the thorax and the abdomen extend beyond the valves (Fig. 8.3, 8.4), except where the carapace is flipped forward. Where the anteriormost part of the thorax is exposed (Figs. 8.8–8.10, 9.7, 9.8) it appears poorly preserved, suggesting that the cuticle normally protected by the carapace was lightly sclerotized and more prone to decay. The thoracic segments bear appendages, whereas the abdomen is apodous. The nature of the preservation does not reveal details of the thoracic appendages, but there is evidence of an elongate branch that tapers distally, terminating in a point. Podomere boundaries are not preserved. This branch, presumably the endopod, extends beyond the continuous outline of the appendages (Figs. 8.5, 8.6, 8.8–8.10, 9.5, 9.6), which probably indicates the extent of overlapping flap-like exopods. Thus, although the detailed nature of the appendages is unknown, they appear to be biramous.

The trunk segment boundaries are fringed by spines, which are occasionally preserved in outline at the trunk margin (Figs. 8.1–8.4, 9.3, 9.4). The boundaries between thoracic segments are usually poorly preserved, particularly at the anterior of the trunk. Where they are evident (Figs. 8.1, 8.2, 9.3–9.8), the posterior thoracic segments appear to be roughly equal in length. The number of segments can be estimated by assuming that there was one pair of appendages per segment, although there may have been more, as in *Branchiocaris pretiosa* (Resser, 1929) (Briggs, 1976). Small relief structures corresponding to thoracic segments (Figs. 8.1, 8.2, 9.5, 9.6) may represent the attachment sites of appendages. The outline of the appendages is never clear, but extrapolation based on their apparent outline in YPM IP 543316 (Fig. 8.3, 8.4) indicates >30, and based on trunk segment divisions, limbs, and attachment sites in YPM IP 239148 (Fig. 9.5, 9.6), >37.

The segments of the abdomen differ from those of the thorax in their greater length and lack of limbs. Identifying the boundary between thorax and abdomen is difficult because there is no abrupt change in the length of segments and the limbs often project posteriorly, overlapping the abdomen. There are at least four, probably five, abdominal segments (Figs. 8.1–8.4, 9.5, 9.6).

The telson is poorly preserved and details are often obscured by superimposition of associated appendages as a result of flattening of the specimens in lateral aspect. A triangular dorsal projection (Fig. 8.3, 8.4), which represents
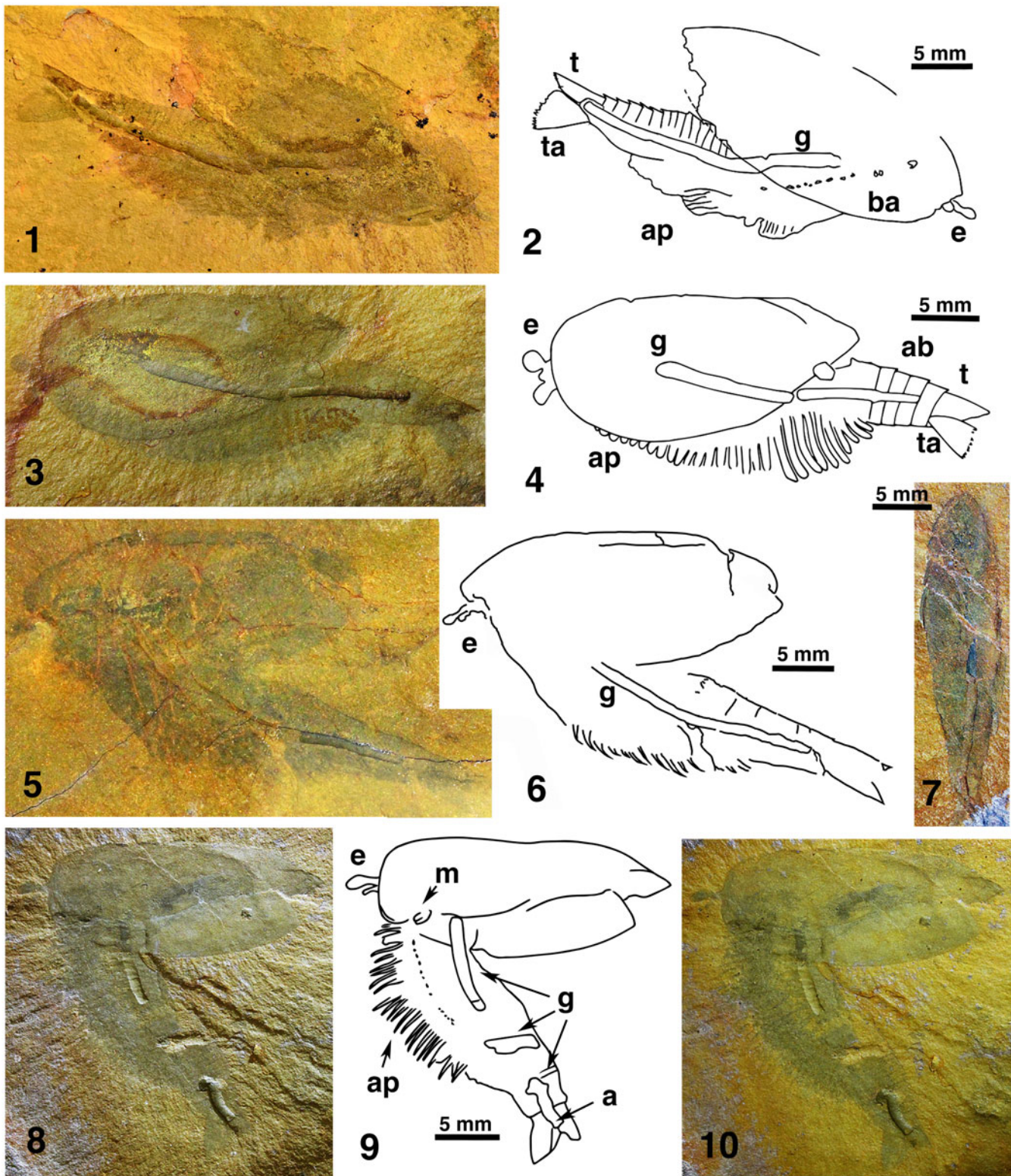
Figure 8. *Vermontcaris montcalmi* n. gen. n. sp. (**1, 2**) YPM IP 543320, holotype, specimen and explanatory drawing. (**3, 4**) YPM IP 543316, specimen and explanatory drawing. (**5, 6**) YPM IP 543333, specimen and explanatory drawing. (**7**) YPM IP 239153. (**8–10**) YPM IP 543334, specimen dry, explanatory drawing, and specimen wet. a = anus; ab = abdomen; ap = thoracic appendages; ba = serially repeated structures indicating limb bases; e = eye; g = gut trace; m = paired relief structures indicating mouth appendages; t = telson; ta = leaf like appendage associated with telson.

the telson, appears to bear some spines ventrally (Fig. 8.1, 8.2). The anus lies ventral of this projection in the more proximal part of the telson (Fig. 9.7, 9.8). A pair of leaf-like appendages, fringed with fine spines (Fig. 8.1–8.4), appears to articulate with the ventral portion of the pre-telson segment (Fig. 8.1–8.4).

Etymology.—In honor of the Montcalm family on whose property the quarry lies.

Material.—YPM IP 543320 holotype, USNM 15314D–F, USNM 15314 G (three poorly preserved specimens), YPM IP 239148, YPM IP 543312, YPM IP 543313, YPM IP 543316, YPM IP 543318–543322, YPM IP 543324, YPM IP 543325, YPM IP 543333–543335, YPM IP 239153.

Dimensions.—Total length (from the anterior of the carapace to the posterior margin of the telson) is difficult to measure accurately due to the curvature of many specimens. It ranges from ∼26 mm (Figs. 8.7–8.9, 9.9, 9.10) to ∼40 mm (Figs. 7.5, 7.6, 8.5, 8.6). Different specimens, however, preserve the shortest and longest valve lengths, which range from ∼20 mm (Fig. 9.1–9.4) to 28 mm (Fig. 8.1, 8.2). The ratio of carapace length to total length (from anterior of carapace to posterior margin of telson head) ranges from 0.60 (Fig. 8.5, 8.6) to 1.05 (Fig. 9.9, 9.10), emphasizing the effect of flattening. YPM IP 543312 (Fig. 9.3, 9.4) falls within this range at 0.64, but the outline of the valve is anomalous. The height of the valve is 16 mm, substantially greater than in any other specimen, and the height to length ratio is 0.89, much greater than the mean of ∼0.5. It is likely that this reflects orientation during flattening. The preserved ratio of valve height to length varies from 0.38 (USNM 15314F and YPM IP 543321) (Figs. 7.5, 7.6, 9.9, 9.10) to 0.89 (YPM IP 543312) (Fig. 9.3, 9.4). Values of H/L: USNM 15314F = 0.38; YPM IP 543312 = 0.89; YPM IP 543316 = 0.47; YPM IP 543319 = 0.48; YPM IP 543320 = 0.41; YPM IP 543321 = 0.38; YPM IP 543333 = 0.43; YPM IP 543334 = 0.43; YPM IP 543335 = 0.53; YPM IP 239148 = 0.48 (Mean 0.49, s 0.15, N = 10; omitting the outlier, YPM IP 543312, mean 0.44, s 0.05, N = 9).

Preservation.—We use the terminology introduced by Whittington (1971) for Burgess Shale specimens to describe variation in the orientation of specimens of *Vermontcaris montcalmi* n. gen. n. sp. to bedding. Whittington (1971) distinguished lateral, parallel (dorso-ventrally flattened), and oblique (intermediate) specimens. *Vermontcaris montcalmi* n. gen. n. sp. is flattened laterally or slightly obliquely (Figs. 7, 8.1–8.6, 8.8–8.10, 9), indicating greater hydrodynamic stability of carcasses in this attitude, presumably because the body was relatively narrow and the valves were not highly convex. YPM IP 239153 (Fig. 8.7), which appears to be flattened dorso-ventrally, as indicated by the narrow carapace and lack of evidence of appendages projecting laterally beyond the trunk, is an exception (a poorly preserved specimen on USNM 15314 G is similar). Specimens show little direct evidence of decay and disarticulation. The carapace is flipped forward in some examples (Figs. 8.5, 8.6, 8.8–8.10, 9.5–9.10) in an attitude that may correspond to the onset of molting (specimens of *Canadaspis perfecta* [Walcott, 1912] [Walcott, 1912a] from the Burgess Shale show a similar configuration; Briggs, 1978a, p. 475). All the specimens in question preserve traces of the gut along the length of the trunk, however, indicating that they represent carcasses; there is no evidence that they are preserved in the act of molting (cf., García-Bellido and Collins, 2004; Yang et al., 2019). The

gut in YPM IP 543334 is preserved in relief in three sections (Fig. 8.8–8.10); the middle of these has rotated, suggesting that the content was authigenically cemented within the carcass. Other specimens preserve the gut in relief (Figs. 7, 8, 9.3–9.10), including examples where it is evident even where it is overlain by the carapace (Figs. 8.1–8.4, 9.3, 9.4), indicating early cementation.

Discussion.—The streamlined carapace, flap-like exopods extending beyond the ventral margin of the carapace, and leaf-like appendages associated with the telson suggest that *Vermontcaris montcalmi* n. gen. n. sp. was a swimmer, as were some other Cambrian bivalved arthropods (Fu and Zhang, 2011; Legg and Caron, 2014). The flexible trunk (e.g., Fig. 9.5, 9.6) may have aided in locomotion. The multiple segments and resulting large number of exopods may have provided enhanced respiratory capability in response to low-oxygen conditions, such as those in the Franklin Basin (Pari et al., 2021).

Remarks.—The morphology of *Vermontcaris montcalmi* n. gen. n. sp., which is characterized by an elongate body, bivalved carapace, and multiple short trunk segments, aligns with that of Cambrian stem-group arthropods such as *Jugatacaris* (Fu and Zhang, 2011) and *Pectocaris* (Hou, 1999; Hou et al., 2004; Jin et al., 2021). The number of thoracic segments in *V. montcalmi* n. gen. n. sp. is difficult to determine, but there may be as many as 40. There is a short abdomen of 4 or 5 segments without appendages. The carapace of *Jugatacaris agilis* from the Chengjiang biota has a dorsal keel or blade-like structure, in contrast to that of *V. montcalmi* n. gen. n. sp. The trunk comprises 55–65 segments, including 3–5 apodous segments at the posterior end (Fu and Zhang, 2011). Fu and Zhang (2011, p. 574) did not designate these posteriormost segments as a separate abdomen, acknowledging the difficulty of drawing a distinction between it and the rest of the trunk. The trunks of *Pectocaris spatiosa*, *P. eurypetala* (Hou and Sun, 1988), and *P. inopinata* Jin et al., 2021, have ∼50 segments, but vary in the number that lack appendages: the first two have ∼4, whereas the last, in contrast to *V. montcalmi* n. gen. n. sp., has 11 or 12 making up a distinct abdomen. The telson of *P. spatiosa* Hou, 1999, is unknown (Hou, 1999). The telson of *P. inopinata* bears a pair of lateral appendages distally, whereas *P. eurypetala* has a median as well as lateral flukes (Hou et al., 2004), similar to the arrangement in *Odaraia alata* Walcott, 1912 (Walcott, 1912a). The lateral appendages in *V. montcalmi* n. gen. n. sp., in contrast, appear to articulate with the pretelson segment. Phylogenetic analyses (Legg et al., 2012; Legg and Caron, 2014) resolved *Pectocaris* and *Jugatacaris* within a paraphyletic grade of bivalved forms, which are part of 'Upper' stem-Euarthropoda at the base of the arthropod stem (Ortega-Hernández, 2016). Bivalved forms with multisegmented elongate bodies likely represent a symplesiomorphic morphology that consistently falls within this clade (J. Yang et al., 2016). Aria and Caron (2017) omitted *Jugatacaris* from their analysis but regarded it as a putative member of the hymenocarines, which resolved as stem mandibulates (Vannier et al., 2018, obtained hymenocarines as crown mandibulates). These several

alternative placements might apply equally to *V. montcalmi* n. gen. n. sp., but the lack of preserved details of the appendages prevent its position from being resolved further.

?Phylum Echinodermata/Phylum Hemichordata stem group
?Unranked Clade Cambroernida Caron, Conway Morris, and Shu, 2010
?*Herpetogaster* Caron, Conway Morris, and Shu, 2010

Type species.—*Herpetogaster collinsi* Caron, Conway Morris, and Shu, 2010, Burgess Shale and Stephen Shale formations, Yoho and Kootenay National Parks, British Columbia, Canada.

?*Herpetogaster* sp.
Figure 10.1, 10.2

2021 *Herpetogaster*?; Pari et al., p. 693, fig. 2H.

Description.—YPM IP 239054 (Fig. 10.1, 10.2) is curved sharply through an angle of ~30°. The shorter, wider portion terminates in an array of tentacle-like structures, which are too poorly preserved to reveal details, and presumably represents the head. The bend coincides with a wide area of gut fill that extends to the outer convex margin and may represent the stomach. There is no unequivocal trace of the gut along the length of the trunk in either direction beyond this fill, and therefore no evidence of the position of the mouth or anus. The longer portion of the trunk ends in a blunt round, presumably posterior, termination. Wrinkles parallel to the margin near this posterior end indicate compaction of relief. The margins of the trunk are not clearly defined everywhere, and there is no evidence of segmentation. The specimen is ~80 mm long.

Material.—YPM IP 239054.

Discussion.—Although poorly preserved, the Parker Formation specimen preserves characters that align with *Herpetogaster*, including the worm-like body, prominent gut trace (possibly the stomach), and array of possible tentacles (Pari et al., 2021). The compaction wrinkles are consistent with a tough, flexible integument (Caron et al., 2010, p. 4). The Parker Formation specimen differs from the lower Cambrian genus *Phlogites* from the Chengjiang Lagerstätte of China, to which *Herpetogaster* has been compared (Caron et al., 2010), in lacking a long stolon continuous with the trunk, although such a structure might be concealed by matrix. It is somewhat larger than previously reported specimens of *Herpetogaster* from other localities.

Caron et al. (2010) and Kimmig et al. (2019) provided comprehensive discussions of the possible deuterostome affinity of *Herpetogaster*. Caron et al. (2010) assigned it to an unranked stem group, which they named cambroernids (without a formal cladistic analysis) lying somewhere on the branch leading to Echinodermata and/or Hemichordata; Kimmig et al. (2019) followed their lead. The Parker Formation specimen potentially extends the geographic range of the genus to the opposite margin of the paleocontinent Laurentia.

Remarks.—We tentatively assign the single specimen, YPM IP 239054, to *Herpetogaster*, a genus that was first described by Caron et al. (2010) on the basis of remarkably preserved material from the Burgess Shale and Stephen Shale formations (Cambrian Miaolingian, Wuliuan). The type species, *H. collinsi* Caron, Conway Morris, and Shu, 2010, is a soft-bodied animal with a tentaculate feeding apparatus and worm-like body, which was attached to the substrate by a stalk or stolon. *Herpetogaster collinsi* also has been reported from the Ruin Wash Lagerstätte (Cambrian Series 2, Stage 4) in the Pioche Formation of Nevada (Kimmig et al., 2019), which is similar in age to the Parker Formation. The apparent arrangement of tentacles in the Parker Formation specimen is very different from that in *H. collinsi*, but more similar to that in a second species, *H. haiyanensis* Yang et al., 2020, from the Chengjiang biota (Yang et al., 2020). Confident assignment of the Parker Formation taxon will require discovery of additional specimens.

Phylum Chordata
Subphylum Vertebrata, stem group
Genus *Emmonsaspis* Walcott, 1890

Type species.—*Emmonsaspis cambrensis* (Walcott, 1890), Parker Formation, Parker Quarry, Franklin County, Vermont, USA.

Emmonsaspis cambrensis (Walcott, 1890)
Figure 10.3–10.5

1886 *Diplograptus* ? *simplex* Walcott, part, p. 92, pl. 11, fig. 4a (non fig. 4).
1889 *Phyllograptus*? *simplex* Walcott, part, p. 388.
1890 *Phyllograptus*? *cambrensis* (Walcott), part, p. 604, pl. 59, fig. 3 (non fig. 3a).
1938 *Emmonsaspis cambriensis* (Walcott); Resser and Howell, part, p. 233, pl. 9, fig. 1 (non figs. 2–4).
1993 *Emmonsaspis cambrensis* (Walcott, 1890); Conway Morris, p. 599, pl. 1, figs. 1, 2.
2014 *Metaspriggina* sp.; Conway Morris and Caron, Extended data fig. 6a–d.
2021 *Metaspriggina*; Pari et al., 2021, p. 693, fig. 2E.

Holotype.—USNM 15314A, Parker Formation, Parker Quarry, Franklin County, Vermont, USA. Cambrian Series 2, Stage 4 (Resser and Howell, 1938, pl. 9, fig,1).

Description.—The original specimens are incomplete, but USNM 15314A, which is the largest, preserves ~50 myomeres (Conway Morris and Caron, 2014, Extended data fig. 6b). The eye is evident in USNM 15314C. USNM 15314A preserves dark ventral features (interpreted by Conway Morris and Caron, 2014, Extended data fig. 6b, as the heart and liver). YPM IP 239155 preserves evidence of the eyes (Fig. 10.3, 10.4) and even a distinct central area (interpreted as the eye lens by Conway Morris and Caron, 2014, fig. 1). YPM IP 239155 preserves evidence of ~50 myomeres (Fig. 10.3), but the distal extremity is not evident. A dark area (Fig. 10.3) is preserved in a similar position to that interpreted as the liver by Conway Morris and Caron (2014). YPM IP 543315 (Fig. 10.5) is unusual in being
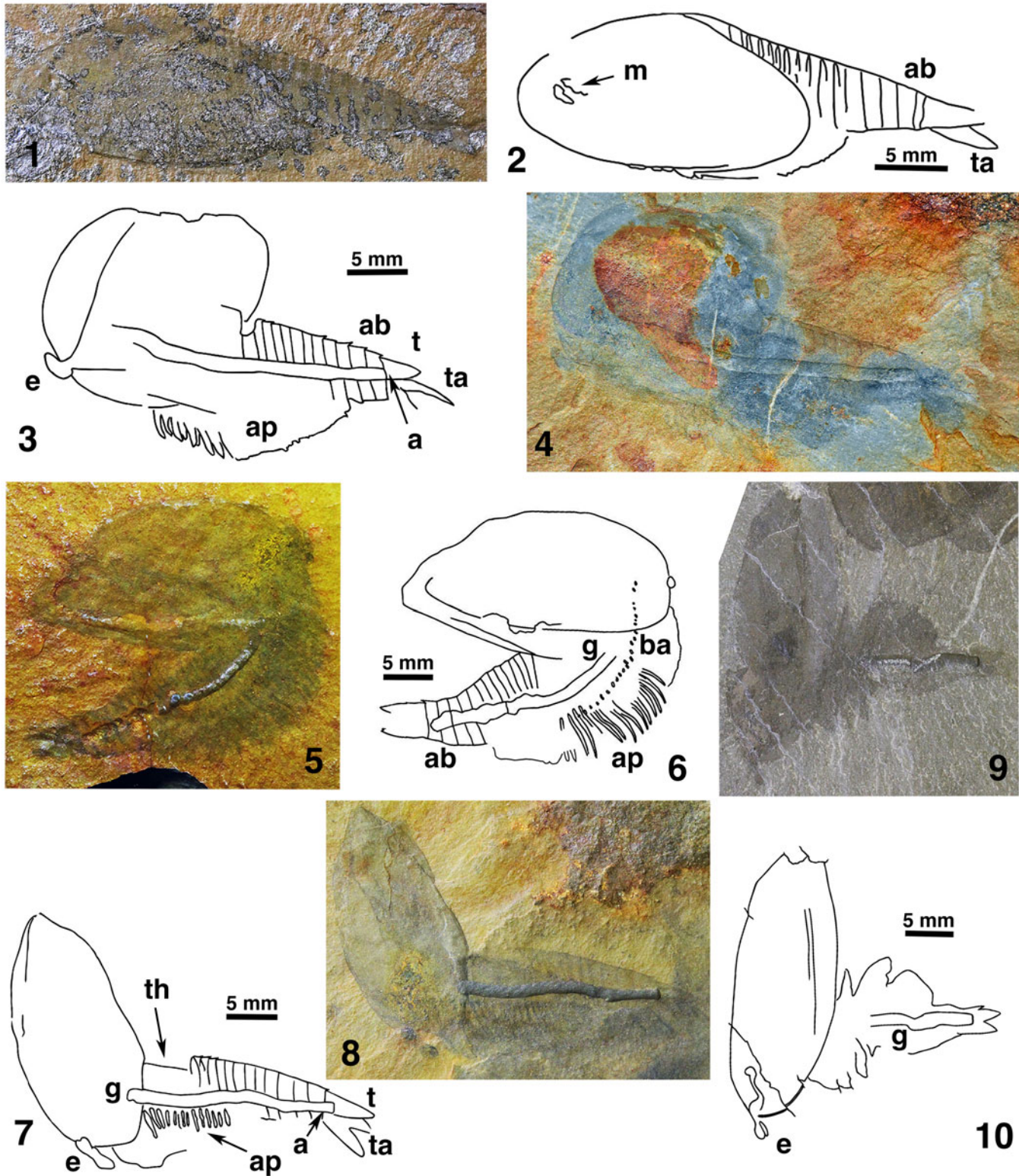
Figure 9. *Vermontcaris montcalmi* n. gen. n. sp. (**1, 2**) YPM IP 543335, specimen and explanatory drawing; (**3, 4**) YPM IP 543312, explanatory drawing and specimen; (**5, 6**) YPM IP 239148, specimen and explanatory drawing; (**7, 8**) YPM IP 543319, explanatory drawing and specimen; (**9, 10**) YPM IP 543321, specimen and explanatory drawing. a = anus; ab = abdomen; ap = thoracic appendages; ba = serially repeated structures indicating limb bases; e = eye; g = gut trace; m = paired relief structures indicating mouth appendages; t = telson; ta = leaf like appendage associated with telson; th = exposed thorax.

preserved as a rust-colored coating, iron oxide presumably after pyrite, that obscures finer details. USNM 15314A was at least 40 mm long and 10 mm high. YPM IP 543315 (Fig. 10.5) was at least 45 mm long. YPM IP 239156 and YPM IP 239155 (Fig. 10.3, 10.4) were at least 35 and 40 mm long, respectively.
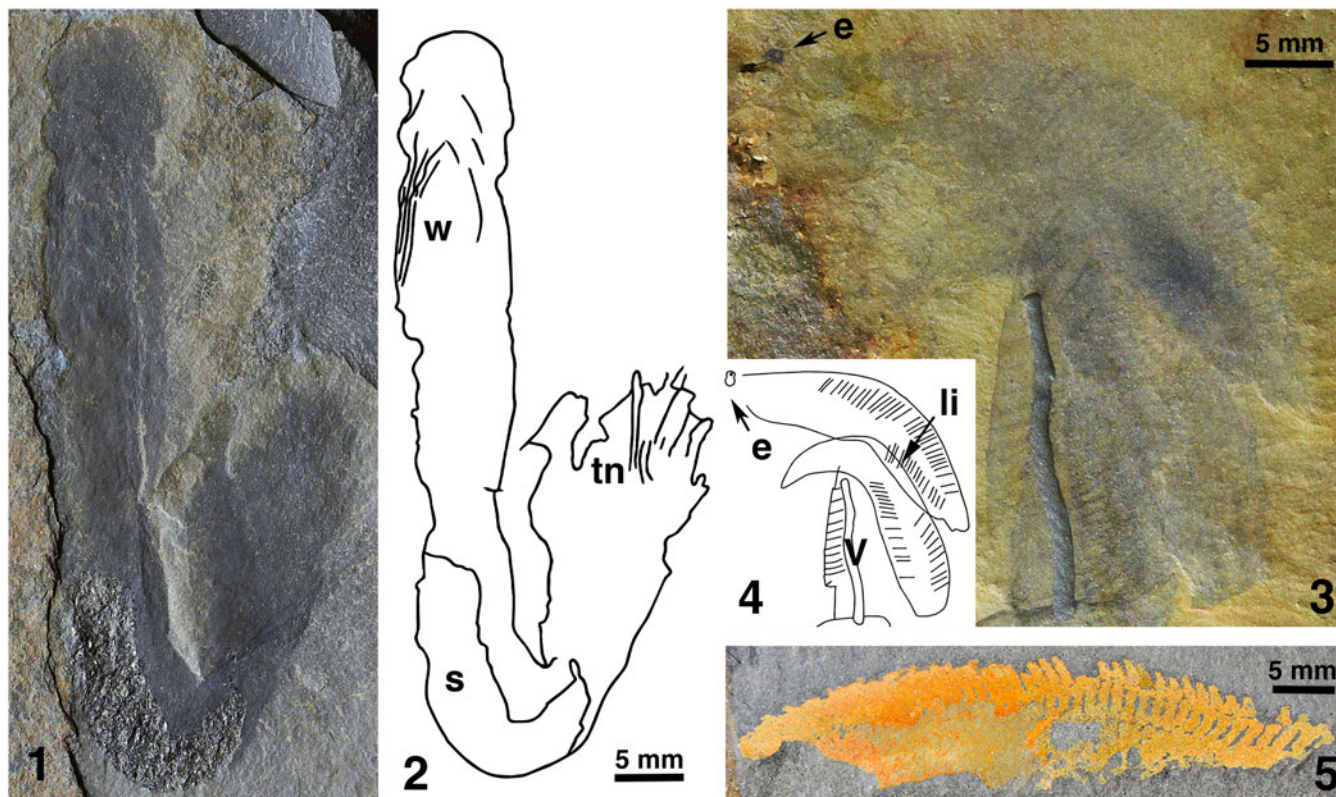
Figure 10. (**1, 2**) ?*Herpetogaster* Caron, Conway Morris, and Shu, 2010, YPM IP 239054, specimen and explanatory drawing. (**3–5**) *Emmonsaspis cambrensis* (Walcott, 1890). (**3, 4**) YPM IP 239155 and YPM IP 239156, two specimens in association with *Vermontcaris montcalmi* n. gen. n. sp. (YPM IP 543319), which is distinguished by the trunk and gut trace (see Fig. 9.8), specimen and explanatory drawing with lines indicating the attitude of the somites; (**5**) YPM IP 543315. e = eye; li = liver; s = stomach; tn = tentacles; V = trunk of *Vermontcaris montcalmi* n. gen. n. sp., YPM IP 543319 (see Fig. 9.8); w = compaction wrinkles.

Material.—USNM 15314A, holotype, USNM 15314B, C, YPM IP 239154-239156, YPM IP 543315, YPM IP 543323.

Discussion.—Conway Morris and Caron (2014) referred the original Parker Formation specimens (well illustrated in their Extended data fig. 6) to *Metaspriggina* spp. without comment. *Metaspriggina* was not named until 1993, when Simonetta and Insom erected a new genus and species from the Burgess Shale, *M. walcotti* Simonetta and Insom, 1993, which was subsequently shown to be a chordate (Conway Morris, 2008). We retain *Emmonsaspis* as the generic name for the Parker Formation taxon, noting that it has priority. Conway Morris and Caron (2014, p. 419) observed that the Parker Formation specimens differ in being less slender and having myomeres with a more angular closure; they also lack evidence of gill bars and zig-zag shaped myomeres. These differences, unless taphonomic, might justify assignment to a separate genus. Otherwise *Metaspriggina* is a junior synonym of *Emmonsaspis*.

Remarks.—Resser and Howell (1938) erected *Emmonsaspis* to accommodate three specimens of this taxon and six specimens that we assign herein to the new taxon, *Vermontcaris montcalmi* n. gen. n. sp., all from the Parker Quarry Lagerstätte, noting (1938, p. 233) that the morphology "of this animal argue[s] strongly for its reference to the chordates." They designated all specimens under USNM 15314 as

cotypes. Conway Morris (1993) initially considered *Emmonsaspis cambrensis* to be a frond-like form similar to some Ediacaran animals. Conway Morris (1993, p. 599) provided a full synonymy of the taxon observing that only the first specimen figured by Resser and Howell (1938, pl. 9, fig. 1), USNM 15314A, is attributable to *E. cambrensis* (Walcott, 1886, pl. 11, fig. 4a; 1890, pl. 59. fig. 3; Conway Morris, 1993, pl. 1, fig. 1). He also noted that the other specimens represent a bivalved arthropod (here described as *V. montcalmi* n. gen. n. sp.). He therefore designated USNM 15314A as holotype (Conway Morris 1993, p. 600) (i.e., lectotype; ICZN Article 74.1), noting its association with two other less well-preserved specimens (USNM 15314B, C). Conway Morris and Caron (2014, Extended Data fig. 6) reinterpreted *E. cambrensis* from the Parker Formation as a chordate as part of their redescription of the chordate *Metaspriggina walcotti* Simonetta and Insom, 1993, from the Burgess Shale (Conway Morris, 2008), based on newly discovered material from the Walcott Quarry and Marble Canyon, assigning the Parker Formation chordate specimens to *Metaspriggina* sp.

Discussion and conclusions

Our excavations at Parker's Cobble have yielded a number of new soft-bodied taxa from the locality (Pari et al., 2021),

including *Fuxianospora*, a ?priapulid, a radiodont, and a possible *Herpetogaster*, as well as multiple specimens of known taxa, particularly the new bivalved arthropod described here as *Vermontcaris montcalmi* n. gen. n. sp. The only other significant Lagerstätten of Cambrian Series 2, Stage 4 age on the southern margin of Laurentia occur in the more widely known Kinzers Formation of Pennsylvania (Muscente et al., 2017; Pari et al., 2021). The Kinzers Formation is also dominated by trilobites, but *Olenellus crassimarginatus* Walcott, 1910, is one of very few that are common to both it and the Parker Formation (Webster and Landing, 2016). Non-biomineralized taxa that occur in both the Kinzers and Parker formations include algae (Skinner, 2005), sponges (Rigby, 1987), possible priapulids (Conway Morris, 1977), radiodonts (Pates and Daley, 2019), *Tuzoia* and other bivalved arthropods (Skinner, 2005), and *Emmonsaspis* (Conway Morris and Caron, 2014). The Kinzers fauna is much more diverse, however, reflecting a greater variety of sedimentary facies, a much greater abundance of fossils, both softbodied and shelly (e.g., echinoderms), and extensive collecting over many years (Thomas, 2021). The Parker Formation also shares taxa with the similarly aged Comet Shale Member of the Pioche Formation of Nevada (Lieberman, 2003), which is on the northern margin of Laurentia, also a muddy bottom setting. The rarity of soft-bodied fossils from the Parker Formation limits meaningful comparisons, an issue that may be resolved by more collecting at the site.

Acknowledgments

References

Aguinaldo, A.M.A., Turbeville, J.M., Linford, L.S., Rivera, M.C., Garey, J.R., Raff, R.A., and Lake, J.A., 1997, Evidence for a clade of nematodes, arthropods and other moulting animals: Nature, v. 387, p. 489–493.

Aitken, J.D., 1997, Stratigraphy of the middle Cambrian platformal succession, southern Rocky Mountains: Geological Survey of Canada Bulletin, v. 398, p. 1–322.

Allison, P.A., 1986, Soft-bodied animals in the fossil record: the role of decay in fragmentation during transport: Geology, v. 14, p. 979–981.

Anderson, R.P., Tosca, N.J., Saupe, E.E., Wade, J., and Briggs, D.E.G., 2021, Early formation and taphonomic significance of kaolinite associated with Burgess Shale fossils: Geology, v. 49, p. 355–359.

Aria, C., and Caron, J.-B., 2017, Burgess Shale fossils illustrate the origin of the mandibulate body plan: Nature, v. 545, p. 89–92.

Aria, C., Caron, J.-B., and Gaines, R., 2015, A large new leanchoiliid from the Burgess Shale and the influence of inapplicable states on stem arthropod phylogeny: Palaeontology, v. 58, p. 629–660.

Bath Enright, O., Minter, N.J., Sumner, E.J., Mángano, M.G., and Buatois L.A., 2021, Flume experiments reveal flows in the Burgess Shale can sample and transport organisms across substantial distances: Communications, Earth and Environment, v. 2, 104. https://doi.org/10.1038/s43247-021-00176-w.

Botting, J.P., 2021, Hexactins in the 'protomonaxonid' sponge *Choiaella* and the proposal of Ascospongiae (class nov.) as a formal replacement for the Protomonaxonida: Bulletin of Geosciences, v. 96, p. 265–277.

Botting, J.P., and Muir, L.A., 2018, Early sponge evolution: a review and phylogenetic framework: Palaeoworld, v. 27, p. 1–29.

Briggs, D.E.G., 1976, The arthropod *Branchiocaris* n. gen., middle Cambrian, Burgess Shale, British Columbia: Geological Survey of Canada Bulletin, v. 264, p. 1–29.

Briggs, D.E.G., 1977, Bivalved arthropods from the Cambrian Burgess Shale of British Columbia: Palaeontology, v. 20, p. 595–621.

Briggs, D.E.G., 1978a, The morphology, mode of life, and affinities of *Canadaspis perfecta* (Crustacea: Phyllocarida), middle Cambrian, Burgess Shale, British Columbia: Philosophical Transactions of the Royal Society B, v. 281, p. 439–487.

Briggs, D.E.G., 1978b A new trilobite-like arthropod from the lower Cambrian Kinzers Formation, Pennsylvania: Journal of Paleontology, v. 52, p. 132–140.

Briggs, D.E.G., 1979, *Anomalocaris*, the largest known Cambrian arthropod: Palaeontology, v. 22, p. 631–664.

Broce, J.S., and Schiffbauer, J.D., 2017, Taphonomic analysis of Cambrian vermiform fossils of Utah and Nevada, and implications for the chemistry of Burgess Shale-type preservation: Palaios, v. 32, p. 600–619.

Budd, G.E., 2008, Head structure in upper stem-group euarthropods: Palaeontology, v. 51, p. 561–573.

Butterfield, N.J., 2002, *Leanchoilia* guts and the interpretation of threedimensional structures in Burgess Shale-type fossils: Paleobiology, v. 28, p. 155–171.

Butterfield, N.J., Balthasar, U., and Wilson, L.A., 2007, Fossil diagenesis in the Burgess Shale: Palaeontology, v. 50, p. 537–543.

Campbell, L.D., 1971, Occurrence of "*Ogygopsis* shale" fauna in southeastern Pennsylvania: Journal of Paleontology, v. 45, p. 437–440.

Caron, J.-B., Conway Morris, S., and Shu, D.-G., 2010, Tentaculate fossils from the Cambrian of Canada (British Columbia) and China (Yunnan) interpreted as primitive deuterostomes: PloS One, v. 5, e9586. https://doi.org/10.1371/journal.pone.0009586.

Chen, J.Y., and Zhou, G., 1997, Biology of the Chengjiang fauna: Bulletin of the National Museum of Natural Science, v. 10, p. 11–105.

Chlupác, I., and Kordule, V., 2002, Arthropods of Burgess Shale type from the middle Cambrian of Bohemia (Czech Republic): Bulletin of the Czech Geological Survey, v. 77, p. 167–182.

Collins, D., 1996, The "evolution" of *Anomalocaris* and its classification in the arthropod Class Dinocarida (nov.) and Order Radiodonta (nov.): Journal of Paleontology, v. 70, p. 280–293.

Cong, P.-Y., Ma, X., Hou, X.-G., Edgecombe, G.D., and Strausfeld, N.J., 2014, Brain structure resolves the segmental affinity of anomalocaridid appendages: Nature, v. 513, p. 538–542.

Cong, P-Y, Edgecombe, G.D., Daley, A.C., Guo, J., Pates, S., and Hou, X.-G., 2018, New radiodonts with gnathobase-like structures from the Cambrian Chengjiang biota and implications for the systematics of Radiodonta: Papers in Palaeontology, v. 4, p. 605–621.

Conway Morris, S., 1977, Fossil priapulid worms: Special Papers in Palaeontology, v. 20, 95 p.

Conway Morris, S., 1986, The community structure of the middle Cambrian Phyllopod Bed (Burgess Shale): Palaeontology, v. 29, p. 423–467.

Conway Morris, S., 1989, The persistence of Burgess Shale-type faunas: implications for the evolution of deeper-water faunas: Transactions of the Royal Society of Edinburgh: Earth Sciences, v. 80, p. 271–283.

Conway Morris, S., 1993, Ediacaran-like fossils in Cambrian Burgess Shaletype faunas of North America: Palaeontology, v. 36, p. 593–635.

Conway Morris, S., 2008, A redescription of a rare chordate, *Metaspriggina walcotti* Simonetta and Insom, from the Burgess Shale (middle Cambrian), British Columbia, Canada: Journal of Paleontology, v. 82, p. 424–430.

Conway Morris, S., and Caron, J.-B., 2014, A primitive fish from the Cambrian of North America: Nature, v. 512, p. 419–422.

Daley, A.C., and Budd, G.E., 2010, New anomalocaridid appendages from the Burgess Shale, Canada: Palaeontology, v. 53, p. 721–738.

Delage, Y., and Hérouard, E., 1897, Les vermidiens: Traités de Zoologie Concrete, v. 5, p. 1–372.

de Laubenfels, M.W., 1955, Porifera, *in* Moore, R.C., ed., Treatise on Invertebrate Paleontology, Part E, Archaeocyatha and Porifera: Boulder, Colorado and Lawrence, Kansas, Geological Society of America and University of Kansas Press, p. E21–E112.

Edgecombe, G.D., Ma, X., and Strausfeld, N.J., 2015, Unlocking the early fossil record of the arthropod central nervous system: Philosophical Transactions of the Royal Society B, v. 370, 20150038. https://doi.org/10.1098/rstb.2015.0038.

Finks, R.M., 1960, Late Paleozoic sponge faunas of the Texas region. The siliceous sponges: Bulletin of the American Museum of Natural History, v. 120, p. 1–160.

Fu, D., and Zhang, X., 2011, A new arthropod *Jugatacaris agilis* n. gen. n. sp. from the early Cambrian Chengjiang Biota, South China: Journal of Paleontology, v. 85, p. 567–586.

Gabbott, S.E., Hou, X.-G., Norry, M.J., and Siveter, D.J., 2004, Preservation of early Cambrian animals of the Chengjiang biota: Geology, v. 32, p. 901–904.

Gaines, R.R., 2014, Burgess Shale-type preservation and its distribution in space and time: Paleontological Society Papers, v. 20, p. 123–146.

Gaines, R.R., and Droser, M.L., 2010, The paleoredox setting of Burgess Shale-type deposits: Palaeogeography, Palaeoclimatology, Palaeoecology, v. 297, p. 649–661.

Gaines, R.R., Briggs, D.E.G., and Zhao, Y.-L., 2008, Cambrian Burgess Shale-type deposits share a common mode of fossilization. Geology, v. 36, p. 755–758.

García-Bellido, D.C., and Collins, D.H., 2004, Moulting arthropod caught in the act: Nature, v. 429, p. 40.

García-Bellido, D.C., and Conway Morris, S., 1999, New fossil worms from the lower Cambrian of the Kinzers Formation, Pennsylvania, with some comments on Burgess Shale-type preservation: Journal of Paleontology, v. 73, p. 394–402.

García-Bellido, D.C., Gozalo, R., Chirivella Martorell, J.B., and Liñán, E., 2007, The demosponge species *Leptomitus* and a new species from the middle Cambrian of Spain: Palaeontology, v. 50, p. 467–478.

García-Bellido, D.C., Paterson, J.R., Edgecombe, G.D., Jago, J.B., Gehling, J.G. and Lee, M.S. 2009, The bivalved arthropods *Isoxys* and *Tuzoia* with soft-part preservation from the lower Cambrian Emu Bay Shale Lagerstätte (Kangaroo Island, Australia): Palaeontology, v. 52, p. 1221–1241.

Grant, R.E., 1836, Animal kingdom, *in* Todd, R.B., ed., The Cyclopedia of Anatomy and Physiology: London, Sherwood, Gilbert and Piper, v. 1, p. 107–118.

Guo, J., Pates, S., Cong, P., Daley, A.C., Edgecombe, G.D., Chen, T., and Hou, X.-G., 2019, A new radiodont (stem Euarthropoda) frontal appendage with a mosaic of characters from the Cambrian (Series 2, Stage 3) Chengjiang Biota: Papers in Palaeontology, v. 5, p. 99–110.

Hagadorn, J.W., 2002, Burgess Shale-type localities: the global picture, *in* Bottjer, D.J., Etter, W., Hagadorn, J.W., and Tang, C.M., Exceptional Fossil Preservation—A Unique View on the Evolution of Marine Life: New York, Columbia University Press, p. 91–116.

Hall, J., 1859, Trilobites of the shales of the Hudson-River Group. Twelfth Annual Report of the Regents of the University of the State of New York, on the condition of the State Cabinet of Natural History, and the Historical and Antiquarian Collection connected therewith: p. 59–62.

Hinde, G.J., 1887, A monograph of the British fossil sponges, Part 1: London, printed for the Palaeontographical Society, Adlard and Son, p. 1–92.

Hou, X.-G., 1999, New rare bivalved arthropods from the lower Cambrian Chengjiang fauna, Yunnan, China: Journal of Paleontology, v. 73, p. 102–116.

Hou, X.-G., and Sun., W.-G., 1988., Discovery of Chengjiang fauna at Meichucun, Jinning, Yunnan: Acta Palaeontologica Sinica, v. 27, p. 1–12. [in Chinese with English summary]

Hou, X.-G., Bergström, J., and Xu, G.-H., 2004, The lower Cambrian crustacean *Pectocaris* from the Chengjiang biota, Yunnan, China: Journal of Paleontology, v. 78, p. 700–708.

Hou X.-G., Siveter, D.J., Siveter, D.J., Aldridge, R.J., Cong, P, Gabbott, S.E. Ma, X, Purnell, M.A., and Williams, M., 2017., The Cambrian Fossils of Chengjiang, China: The Flowering of Early Animal Life, 2nd Ed.: Oxford, UK, Wiley, 328 p.

Howard, R.J., Edgecombe, G.D., Shi, X.-M., Hou, X.-G., and Ma, X.-Y., 2020, Ancestral morphology of Ecdysozoa constrained by an early Cambrian stem group ecdysozoan: BMC Evolutionary Biology, v. 20, 156. https://doi.org/10.1186/s12862-020-01720-6.

Jin, C., Mai, H., Chen, H., Liu, Y., Hou, X., Wen, R., and Zhai, D., 2021, A new species of the Cambrian bivalved euarthropod *Pectocaris* with axially differentiated enditic armatures: Papers in Palaeontology, v. 7, 1781–1792.

Kimmig, J., Meyer, R.C., and Lieberman, B.S., 2019, *Herpetogaster* from the early Cambrian of Nevada (Series 2, Stage 4) and its implications for the evolution of deuterostomes: Geological Magazine, v. 156, p. 172–178.

Landing, E., 2007, Ediacaran–Ordovician of east Laurentia—Geologic setting and controls on deposition along the New York Promontory region, *in* Landing, E., ed., Ediacaran–Ordovician of East Laurentia—S. W. Ford Memorial Volume. 12th International Conference of the Cambrian Chronostratigraphy Working Group: New York State Museum Bulletin, v. 510, p. 2–24.

Legg, D.A., and Caron, J.-B., 2014, New middle Cambrian bivalved arthropods from the Burgess Shale (British Columbia, Canada): Palaeontology, v. 57, p. 691–711.

Legg, D.A., Sutton, M.D., Edgecombe, G.D., and Caron, J.-B., 2012, Cambrian bivalved arthropod reveals origin of arthrodisation: Proceedings of the Royal Society B, v. 279, p. 4699–4704.

Legg, D.A., Sutton, M.D., and Edgecombe, G.D., 2013, Arthropod fossil data increase congruence of morphological and molecular phylogenies: Nature Communications, v. 5, 2485. https://doi.org/10.1038/ncomms3485.

Lerosey-Aubril, and Pates, S., 2018, New suspension-feeding radiodont suggests evolution of microplanktivory in Cambrian macronekton: Nature Communications, v. 9, 3774. https://doi.org/10.1038/s41467-018-06229-7.

Lerosey-Aubril, R., Kimmig, J., Pates, S., Skabelund, J., Weug, A., and Ortega-Hernández, J., 2020, New exceptionally preserved panarthropods from the Drumian Wheeler Konservat-Lagerstätte of the House Range of Utah: Papers in Palaeontology, v. 6, p. 501–531.

Lieberman, B.S., 1999, Systematic revision of the Olenelloidea (Trilobita, Cambrian): Bulletin of the Peabody Museum of Natural History Yale University, v. 45, p. 1–150.

Lieberman, B.S., 2003, A new soft-bodied fauna: the Pioche Formation of Nevada: Journal of Paleontology, v. 77, p. 674–690.

LoDuca, S.T., Caron, J.-B., Schiffbauer, J.D., Xiao, S., and Kramer, A., 2015a, A reexamination of *Yuknessia* from the Cambrian of British Columbia and Utah: Journal of Paleontology, v. 89, p. 82–95.

LoDuca, S.T., Wu, M.-Y., Zhao, Y.-L., Xiao, S., Schiffbauer, J.D., Caron, J.-B., and Babcock, L.E., 2015b, Reexamination of *Yuknessia* from the Cambrian of China and first report of *Fuxianospira* from North America: Journal of Paleontology, v. 89, p. 899–911.

LoDuca, S.T., Bykova, N., Wu, M., Xiao, S., and Zhao, Y., 2017, Seaweed morphology and ecology during the great animal diversification events of the early Paleozoic: a tale of two floras: Geobiology, v. 15, p. 588–616.

Marcou, J., 1880, Sur les colonies dans les roches taconiques des bords du lac Champlain: Bulletin de la Société Géologique de France, v. 9, p. 18–46.

Marcou, J., 1888, The Taconic of Georgia and the report on the geology of Vermont: Boston Society of Natural History Memoirs, v. 4, p. 105–131.

Miller, S.A., 1889, North American Geology and Palaeontology for the use of amateurs, students and scientists: Cincinnati, Western Methodist Book Concern, 664 p.

Moysiuk, J., and Caron, J.-B., 2021, Exceptional multifunctionality in the feeding apparatus of a mid-Cambrian radiodont: Paleobiology, v. 47, p. 704–724.

Muscente, A.D., Schiffbauer, J.D., Broce, J., Laflamme, M., O'Donnell, K., et al., 2017, Exceptionally preserved fossil assemblages through geologic time and space: Gondwana Research, v. 48, p. 164–188.

Nanglu, K., and Caron, J.-B., 2018, A new Burgess Shale polychaete and the origin of the annelid head revisited: Current Biology, v. 28, p. 319–326.

Nielsen, C., 1995, Animal Evolution: Interrelationships of the Living Phyla: Oxford, UK, Oxford University Press, 467 p.

Orr, P.J., Briggs, D.E.G., and Kearns, S.L., 1998, Cambrian Burgess Shale animals replicated in clay minerals: Science, v. 281, p. 1173–1175.

Ortega-Hernández, J., 2016, Making sense of 'lower' and 'upper' stem-group Euarthropoda, with comments on the strict use of the name Arthropoda von Siebold, 1848: Biological Reviews, v. 91, p. 255–273.

Pari, G., Briggs, D.E.G., and Gaines, R.R., 2021, The Parker Quarry Lagerstätte of Vermont—the first reported Burgess Shale-type fauna rediscovered: Geology, v. 49, p. 693–697.

Pates, S., and Daley, A.C., 2019, The Kinzers Formation (Pennsylvania, USA): the most diverse assemblage of Cambrian Stage 4 radiodonts: Geological Magazine, v. 156, p. 1233–1246.

Pates, S., Daley, A.C., Edgecombe, G.D., Cong, P., and Lieberman, B.S., 2021, Systematics, preservation, and biogeography of radiodonts from the southern Great Basin, USA, during the Upper Dyeran (Cambrian Series 2, Stage 4): Papers in Palaeontology, v. 7, p. 235–262.

Ramírez-Guerrero, G.M., and Cameron, C.B., 2021, Systematics of pterobranchs from the Cambrian Period Burgess Shales of Canada and the early evolution of graptolites: Bulletin of Geosciences, v. 96, p. 1–18.

Ratcliffe, N.M., Stanley, R.S., Gale, M.H., Thompson, P.J., and Walsh, G.J., 2011, Bedrock geologic map of Vermont: U.S. Geological Survey Scientific Investigations Map 3184, 3 sheets, scale 1:100,000.

Raymond, P.E., 1935, *Leanchoilia* and other mid-Cambrian Arthropoda: Bulletin of the Museum of Comparative Zoology, Harvard University, v. 76, p. 205–230.

Reid, R.E.H., 1958, A monograph of the Upper Cretaceous Hexactinellida of Great Britain and Northern Ireland: Palaeontographical Society of London, Part 1, p. 1–46.

Resser, C.E., 1929, New lower and middle Cambrian Crustacea: Proceedings of the U.S. National Museum, v. 76, p. 1–18.

Resser, C.E., and Howell, B.F., 1938, Lower Cambrian *Olenellus* Zone of the Appalachians: Bulletin of the Geological Society of America, v. 49, p. 195–248.

Rigby, J.K., 1986, Sponges of the Burgess Shale (Middle Cambrian), British Columbia: Palaeontographica Canadiana, v. 2, 105 p.

Rigby, J.K., 1987, Early Cambrian sponges from Vermont and Pennsylvania, the only ones described from North America: Journal of Paleontology, v. 61, p. 451–461.

Rigby, J.K., and Collins, D., 2004, Sponges of the middle Cambrian Burgess Shale and Stephen formations, British Columbia: Royal Ontario Museum Contributions in Science, v. 1, p. 1–155.

Salter, J.W., 1864, On some new fossils from the *Lingula*-flags of Wales: Quarterly Journal of the Geological Society of London, v. 20, p. 233–241.

Sansom, R.S., 2016, Preservation and phylogeny of Cambrian ecdysozoans tested by experimental decay of *Priapulus*: Scientific Reports, v. 6, 32817. https://doi.org/10.1038/srep32817.

Schiffbauer, J.D., Xiao, S., Cai, Y., Wallace, A.F., Hua, H., Hunter, J., Xu, H., Peng, Y., and Kaufman, A.J., 2014, A unifying model for Neoproterozoic–Palaeozoic exceptional fossil preservation through pyritization and carbonaceous compression: Nature Communications, v. 5, 5754. https://doi.org/10.1038/ncomms6754.

Schmidt, O., 1870, Grundzüge einer Spongien-Fauna des Atlantischen Gebietes: Leipzig, Wilhelm Engelmann, 88 p.

Shaw, A.B., 1954, Lower and lower middle Cambrian faunal succession in northwestern Vermont: Bulletin of the Geological Society of America, v. 65, p. 1033–1046.

Shaw, A.B., 1955, Paleontology of northwestern Vermont. V. The lower Cambrian fauna: Journal of Paleontology, v. 29, p. 775–805.

Simonetta, A.M., and Delle Cave, L., 1975, The Cambrian nontrilobite arthropods from the Burgess Shale of British Columbia. A study of their comparative morphology, taxonomy and evolutionary significance: Palaeontographia Italica, v. 69, p. 1–37.

Simonetta, A.M., and Insom, E., 1993, New animals from the Burgess Shale (middle Cambrian) and their possible significance for the understanding of the Bilateria: Bollettino di Zoologia, v. 60, p. 97–107.

Skinner, E.S., 2005, Taphonomy and depositional circumstances of exceptionally preserved fossils from the Kinzers Formation (Cambrian), southeastern Pennsylvania: Palaeogeography, Palaeoclimatology, Palaeoecology, v. 220, p. 167–192.

Smith, M.R., Harvey, T.H.P., and Butterfield, N.J., 2015, The macro- and microfossil record of the Cambrian priapulid *Ottoia*: Palaeontology, v. 58, p. 705–721.

Thomas, R.D.K., 2021, Documentation by citizen scientists/naturalists of the 'Cambrian explosion' in Pennsylvania: Geology Today, v. 37, 57–62.

Vannier, J., Caron, J.-B., Yuan, J.-L., Briggs, D.E.G., Collins, D., Zhao, Y.-L., and Zhu, M.-Y., 2007, *Tuzoia*: morphology and lifestyle of a large bivalved arthropod of the Cambrian seas: Journal of Paleontology, v. 81, p. 445–471.

Vannier, J., Aria, C., Taylor, R.S., and Caron, J.-B., 2018, *Waptia fieldensis* Walcott, a mandibulate arthropod from the middle Cambrian Burgess Shale: Royal Society Open Science, v. 5, 172206. https://doi.org/10.1098/rsos.172206.

Van Roy, P., Daley, A.C., and Briggs, D.E.G., 2015, Anomalocaridid trunk limb homology revealed by a giant filter-feeder with paired flaps: Nature. v. 522, p. 77–80.

Vinther, J., Stein, M., Longrich, N.R., and Harper, D.A.T., 2014, A suspension-feeding anomalocarid from the Early Cambrian: Nature, v. 507, p. 496–499.

Walcott, C.D., 1884, On a new genus and species of Phyllopoda from the middle Cambrian, *in* Walcott, C.D., On the Cambrian Faunas of North America —Preliminary studies: United States Geological Survey Bulletin, v. 10, p. 50–51, 74–75.

Walcott, C.D., 1885, New genus of Cambrian trilobites, *Mesonacis*: American Journal of Science, v. 29, p. 328–330.

Walcott, C.D., 1886, Second contribution to the studies on the Cambrian faunas of North America: United States Geological Survey Bulletin, v. 30, 369 p.

Walcott, C.D., 1889, Stratigraphic position of the *Olenellus* fauna in North America and Europe: American Journal of Science, v. 37, p. 374–392, v. 38, p. 29–42.

Walcott, C.D., 1890, The fauna of the Lower Cambrian or *Olenellus* Zone: Tenth Annual Report of the Director, 1888–1889, United States Geological Survey, p. 509–774.

Walcott, C.D., 1910, *Olenellus* and other genera of the Mesonacidae: Cambrian Geology and Paleontology, Smithsonian Miscellaneous Collections, v. 53, p. 231–422.

Walcott, C.D., 1911a, Middle Cambrian Merostomata: Cambrian Geology and Paleontology II, Smithsonian Miscellaneous Collections, v. 57, p. 17–40.

Walcott, C.D., 1911b, Middle Cambrian annelids: Cambrian Geology and Paleontology II, Smithsonian Miscellaneous Collections, v. 57, p. 109–134.

Walcott, C.D., 1912a, Middle Cambrian Branchiopoda, Malacostraca, Trilobita and Merostomata: Cambrian Geology and Paleontology II, Smithsonian Miscellaneous Collections, v. 57, p. 145–228.

Walcott, C.D., 1912b, Cambrian Brachiopoda: United States Geological Survey Monograph, v. 51, pt. 1, 872 p.

Walcott, C.D., 1919, Middle Cambrian algae: Cambrian Geology and Paleontology IV, Smithsonian Miscellaneous Collections, v. 67, p. 217–260.

Walcott, C.D., 1920, Middle Cambrian spongiae: Cambrian Geology and Paleontology IV, Smithsonian Miscellaneous Collections, v. 67, p. 261–364.

Wang, P.-L., LoDuca, S.T., Wu, M.Y., Tang, Y.-G., and Sun, Z.-X., 2021, in press, Benthic primary producers in exceptionally preserved Cambrian biotas of North China: Palaeoworld. https://doi.org/10.1016/j.palwor.2021.01.009.

Webster, M., 2009, Systematic revision of the Cambrian trilobite *Bathynotus* Hall, 1860, with documentation of new occurrences in western Laurentia and implications for intercontinental biostratigraphic correlation: Memoirs of the Association of Australasian Palaeontologists, v. 37, p. 369–406.

Webster, M., and Landing, E., 2016, Geological context, biostratigraphy and systematic revision of late early Cambrian olenelloid trilobites from the Parker and Monkton formations, northwestern Vermont, U.S.A.: Australasian Palaeontological Memoirs, v. 49, p. 193–240.

Wen, R.-Q., Zhao, Y.-L., and Peng, J., 2015, Morphology and ontogeny of *Tuzoia bispinosa* from the Kaili Biota (Cambrian Stage 5) of eastern Guizhou, China: Palaeoworld, v. 24, p. 61–70.

Wen, R.-Q., Babcock, L.E., Peng, J., Liu, S., and Liang, B., 2019, The bivalved arthropod *Tuzoia* from the Balang Formation (Cambrian Stage 4) of Guizhou, China, and new observations on comparative species: Papers in Palaeontology, v. 5, p. 719–742.

Whittington, H.B., 1971, The Burgess Shale: history of research and preservation of fossils: Proceedings of the North American Paleontological Convention 1969, Lawrence, Kansas, Allen Press, v. I, p. 1170–1201.

Whittington, H.B., 1988, Hypostomes and ventral cephalic sutures in Cambrian trilobites: Palaeontology, v. 31, p. 577–609.

Whittington, H.B., 1989, Olenelloid trilobites: type species, functional morphology and higher classification: Philosophical Transactions of the Royal Society of London B, v. 324, p. 111–147.

Yang, J., Ortega-Hernández, J., Lan, T., Hou, J., and Zhang, X., 2016, A predatory bivalved euarthropod from the Cambrian (Stage 3) Xiaoshiba Lagerstätte, South China: Scientific Reports, v. 6, 27709. https://doi.org/10.1038/srep27709.

Yang, J., Ortega-Hernández, J., Drage, H.B., Du, K., and Zhang, X., 2019, Ecdysis in a stem-group euarthropod from the early Cambrian of China: Scientific Reports, v. 9, 5709. https://doi.org/10.1038/s41598-019-41911-w.

Yang, X., Kimmig, J., Lieberman, B.S., and Peng, S., 2020, A new species of the deuterostome *Herpetogaster* from the early Cambrian Chengjiang biota of South China: Naturwissenschaften, v. 107, 37. https://doi.org/10.1007/s00114-020-01695-w.

Yang, Y., Zhao, Y., and Zhang, X., 2016, Fossil priapulid *Ottoia* from the Kaili biota (Cambrian Series 3) of South China: Journal of Systematic Palaeontology, v. 14, p. 527–543.

Yochelson, E.L., 1998, Charles Doolittle Walcott, Paleontologist: Kent, Ohio, The Kent State University Press, 510 p.